Tsunami's Impact on Palu, Indonesia: A Geospatial Assessment of Affected Zones by 2018 Sulawesi Earthquake & Tsunami

A thesis submitted by

Youshuang Hu

In partial fulfillment of the requirement

for the degree of

Master of Science

in

Environmental Policy and Planning

Tufts University

February 2024

Advisor:

Aggeliki Barberopoulou

Reader:

Magaly Koch

ABSTRACT

The 2018 Sulawesi Earthquake and Tsunami serve as a somber backdrop for this thesis, which provides an in-depth geospatial analysis of the calamity's impact on Palu, Indonesia. Through remote sensing and the application of the Analytical Hierarchy Process (AHP), this study maps the extent of the destruction and evaluates the region's vulnerability to such catastrophic events. It draws upon a rich dataset from satellite imagery to dissect the correlations between topographical features, land use, and the varying degrees of damage observed across the urban landscape.

The thesis advances a multi-criteria decision-making framework that underpins the assessment of vulnerability and risk associated with tsunamis, taking into account the complex interplay between natural and anthropogenic factors. By integrating elevation, slope, coastal proximity, and land use, the research offers a granular perspective on the spatial distribution of tsunami related damages and identifies patterns that are vital for disaster risk reduction strategies.

Moreover, the findings emphasize the urgent need for urban planning that prioritizes resilience, incorporating the nuanced insights gained from geospatial analyses. The study's outcomes are poised to inform policy-making, contributing to the establishment of enhanced early warning systems, optimized evacuation routes, and the strategic placement of infrastructure. The overarching goal is to equip coastal cities like Palu with robust preparedness measures, ensuring a proactive stance against the inevitability of future natural disasters.

In sum, this thesis not only charts the aftermath of one of Indonesia's most significant recent disasters but also lays the groundwork for a more informed and resilient approach to

urban planning and disaster management in similarly vulnerable coastal regions around the world.

ACKNOWLEDGEMENT

When I wrote this, I realized that with the completion of the thesis, my graduate life is about to come to an end. I still remember the joy and nervousness of stepped into Tufts University for the first time. The campus life in the past two years has left me with many precious memories, which I will keep forever. I know this is end, yet it is also another beginning.

First, I would like to show my heartfelt gratitude to my thesis advisor, Dr. Aggeliki Barberopoulou, who provided many valuable suggestions for this thesis. Even in the spare time of busy teaching work, she always answered me questions in a very short time and encouraged me when I encountered difficulties. Then, I would like to express my most sincere thanks to my thesis reader, Dr. Magaly Koch. It is because of her help that I can break through myself again and again and make continuous progress.

I also want to express my thanks to my parents and friends. They have always supported me unconditionally in every decision I made and guided my direction when I was confused. They are superheroes in my heart. At the same time, I want to say something to myself who has been insisting: Please maintain this love, even at the most difficult moments.

We will all have bright futures, in various ways.

TABLE OF CONTENTS

ABSTRACT **2**

ACKNOWLEDGEMENT **4**

LIST OF FIGURES **7**

LIST OF TABLES **9**

CHAPTER 1: INTRODUCTION **10**

CHAPTER 2: LITERATURE REVIEW **15**

2.1 Remote Sensing Techniques in Tsunami Analysis 15
2.2 Analytical Hierarchy Process 17

CHAPTER 3: RESEARCH QUESTIONS **20**

CHAPTER 4: MATERIALS & METHODS **23**

4.1 Study Area 23
4.2 Data 25
4.2.1 Remote Sensing Imagery *25*
4.2.2 Geographic Data *28*
4.3 Methodology 30
4.3.1 Remote Sensing Workflow *30*
4.3.2 Index Formulas *31*
4.3.3 Tsunami Vulnerability Model Workflow *33*

CHAPTER 5: REMOTE SENSING ANALYSIS **35**

5.1 False Color Composite 35
5.2 Computation of Indices 36
5.2.1 Normalized Difference Vegetation Index *36*
5.2.2 Normalized Difference Water Index *38*
5.2.3 Normalized Difference Soil Index *40*
5.3 Threshold Analysis 42
5.4 Tsunami-Affected Areas Based on Thresholds of NDVI, NDSI, and NDWI 45

CHAPTER 6: GEOSPATIAL DATA ANALYSIS **48**

6.1 Topographic Elevation Mapping 48
6.2 Topographic Slope Mapping 50
6.3 Coastal Proximity Mapping 52
6.4 Land Use Mapping 54
6.5 Analytical Hierarchy Process 56
6.6 Tsunami Vulnerability Mapping 59

CHAPTER 7 SUMMARY **62**

7.1 Conclusion 62
7.2 Policy Implications 63
7.3 Limitations 64
7.4 Recommendations for Future Research 64

APPENDIX **66**

APPENDIX 1: FALSE COLOR COMPOSITE **66**

APPENDIX 2: NDVI PRE-TSUNAMI IMAGE (09/27/2018) **67**

APPENDIX 3: NDSI PRE- (09/27/2018) AND POST-TSUNAMI IMAGE (10/02/2018).....69
APPENDIX 4: NDWI PRE- (09/27/2018) AND POST-TSUNAMI IMAGE (10/02/2018).....70
BIBLIOGRAPHY 71

LIST OF FIGURES

Figure 1 Study Area the City of Palu. Data Source: AHA – Indonesia Subnational Administrative Boundary 24

Figure 2 Remote Sensing Workflow 30

Figure 3 Main methodology steps followed for the tsunami vulnerability mapping based on different factors.....33

Figure 4 False Color Composite after tsunami (10/02/2018) (SWIR, VNIR and RED as RGB bands) 35

Figure 5 Reclassification NDVI for pre-tsunami (09/27/2018) (left) and post-tsunami imagery (10/02/2018) (right) 37

Figure 6 Reclassification NDWI for pre-tsunami (09/27/2018) (left) and post-tsunami imagery (10/02/2018) (right) 38

Figure 7 Reclassification NDSI for pre-tsunami (09/27/2018) (left) and post-tsunami imagery (10/02/2018) (right) 40

Figure 8 Computed NDVI, NDSI, and NDWI for pre-tsunami (09/27/2018) and post-tsunami (10/02/2018) in small areas of Palu 43

Figure 9 Cumulative Frequency Distribution of the differences of NDVI, NDSI and NDWI 44

Figure 10 Mapping NDVI, NDSI and NDWI based on the threshold values 45

Figure 11 Final Tsunami Inundation Map based on Decision Tree.....47

Figure 12 Tsunami Vulnerability Map based on Topographic Elevation 49

Figure 13 Tsunami Vulnerability Map based on Topographic Slope 51

Figure 14 Tsunami Vulnerability Map Based on Coastal Proximity 53

Figure 15 Tsunami Vulnerability Map Based on Land Use 55

Figure 16 Tsunami Vulnerability Map based on Elevation, Slope, Coastal Proximity and Land Use

LIST OF TABLES

Table 1 Tsunami Summary in Indonesia 11

Table 2 Sentinel-2 Imagery Description Table 25

Table 3 Maxar WorldView Imagery Description Table 27

Table 4 Topographic Elevation Data.....28

Table 5 Land Use Data.....28

Table 6 Indonesia Administrative Boundary Data 28

Table 7 NDVI Value Calculation for Pre- and Post-tsunami Imagery.....37

Table 8 NDWI Value Calculation for Pre- and Post-tsunami Imagery.....39

Table 9 NDSI Value Calculation for Pre- and Post-tsunami Imagery 40

Table 10 Tsunami Vulnerability based on Topographic Elevation (Lidia, 1963) 48

Table 11 Tsunami Vulnerability based on Topographic Slope (Van Zuidam, 1983).....50

Table 12 Tsunami Vulnerability based on Coastal Proximity.....52

Table 13 Tsunami Vulnerability based on Land Use (Sambah & Miura, 2016).....54

Table 14 Pairwise Comparison Matrix 56

Table 15 Normalized Pairwise Comparison Matrix 57

Table 16 Normalized Pairwise Comparison Matrix + Weight Calculation 58

Table 17 Variable Percentage Table 58

Table 18 Consistency Level Table 59

Table 19 Vulnerability Class Based on Elevation (Iida, 1963), Slope (Van Zuidam, 1983), Coastal Proximity (Bretschneider and Wybro, 1976) and Land Use (Sambah & Miura, 2016) 59

CHAPTER 1: INTRODUCTION

'Tsunamis', often referred to as 'harbor waves' in native Japanese, are geological phenomena of profound significance and impact (Koshimura et al., 2020; Röbke & Vött, 2017; Shuto & Fujima, 2009). These giant waves typically result from a sudden displacement of the water column, triggered by events such as earthquakes, volcanic eruptions, cosmic impacts, or atmospheric disturbances (e.g., Kanamori et al., 1972; Abe, 1973; Röbke & Vött, 2017; Harbitz et al., 2006; Papadopoulos et al., 2016). Tsunamis are characterized by their long wavelengths, which can extend for hundreds of kilometers, and they can travel across entire ocean basins (Jaumé & Sykes, 1999; van Rijsingen et al., 2018; Han et al., 2010; Baba & Cummins, 2005; Thielr & Zsutty et al., 1987). While wave amplitudes are very small in deep ocean (often going unnoticed), it is near shallow coastal areas, that their period "shrinks", while growing in height and can become immensely destructive (e.g., Wesnousky, 2008; Oth, 2013; Van et al., 1984; Løvholt et al., 2015). Tsunamis have the potential to cause widespread devastation through inundation, erosion, strong currents in ports and harbors, scouring caused by strong forces generated during receding of waters, leading to loss of life and property damage. On many occasions (e.g. Tohoku 2011) tsunami caused more damage than the earthquake that caused it.

Indonesia is particularly vulnerable to many geophysical hazards including earthquakes, tsunamis and volcanoes due to its geographic location and tectonic setting. Indonesia's location at a junction of three of tectonic plates (Indo-Australian Plate, the Eurasian Plate and the Pacific Plate), along with numerous underwater volcanoes and a densely populated coastal zone, means that a large part of the country's population is exposed to a number of disasters including

tsunamis as we have observed in the recent past (2004 Banda Aceh tsunami; Reid & Mooney, 2023; Muhari et al., 2007; Esteban et al., 2013; Mutaqin et al., 2019; Supriatna et al., 2018;). However, Indonesia is known for its long history of significant tsunami events. According to the global tsunami database, a total of 77 tsunamis have been documented since 1608. These tsunamis have claimed the lives of more than 368,000 people in the country.[1] Among these, the catastrophic 2004 Indian Ocean tsunami alone killed 167,540 people in Indonesia and more than 220,000 people in 14 countries in Asian and the African continents.[2]

Table 1 Tsunami Summary in Indonesia [3]

Tsunami Name	Date	Source	Location Name	Earthquake Magnitude	Maximum Water Height (m)	Total Deaths
2004 Indian Ocean Tsunami	12/24/2004	Earthquake	Sumatra	9.1	50.9	227899
2005 Nisa-Simeulue Tsunami	03/28/2005	Earthquake	Indonesia	8.6	4.2	1313
2006 Pangandaran Tsunami	07/17/2006	Earthquake	South of Java	7.7	20.9	802
2010 Mentawai Tsunami	10/25/2010	Earthquake	Sumatra	7.8	16.9	431
2018 Sulawesi Tsunami	09/20/2018	Earthquake & Volcano	Sulawesi	7.5	10.73	4340
2018 Sunda strait Tsunami	12/22/2018	Volcano & Landslide	Krakatau		85	437

[1] Data Source: https://www.ngdc.noaa.gov/hazel/view/hazards/tsunami/event-search

[2] Data Source: International Tsunami Information Center http://itic.ioc-unesco.org/index.php

[3] Data Source: https://www.ngdc.noaa.gov/hazel/view/hazards/tsunami/event-search

Preparedness and early warning systems are therefore crucial in order to minimize life loss, something which became more clear post 2004. According to the United Nations Environmental Programme (UNEP) in 2015, the early warning system (EWS) is defined as a structured and integrated set of tools, processes, and communication systems designed to detect, assess, and communicate information about potential hazards or threats in advance of their occurrence (UNEP, 2015). As a result, EWS's goal is to prevent loss of life during the most significant disasters. In Indonesia, the structural EWS has been in operation since the 2004 tsunami in Aceh, regulated under a range of laws and policies related to responsibilities of assorted government at all administrative levels, including information dissemination. However, the early warning system (EWS) introduced in regulations, has not been fully implemented, presenting substantial challenges, particularly concerning budget allocations and government coordination (Atkinson & Curnin, 2020). For instance, in 2018, the Sulawesi Island was struck by a powerful earthquake and tsunami. While the seismic activity was detected, the local EWS capacity to disseminate alerts was insufficient. This resulted in a delayed response, leaving communities in the earthquake and tsunami's trajectory with insufficient time to evacuate, leading a significant loss of life and widespread destruction (Omira et al., 2019; Paulik et al., 2019).

Furthermore, cultural knowledge plays a key role in disaster management in Indonesia. Over centuries, the people of Indonesia have cultivated their own social resilience by generating local knowledge (e.g., 'Smong', 'saur sepuh', and 'pating njlethot') to mitigate disaster risks. An illustrative example can be shown by *'Smong' from Simeuleu Regency* in 2005 Aceh Tsunami (Suciani et al., 2018; Juwitasari et al., 2022). The report published by Juwitasari et al. (2022) documented that:

*"In the tsunami that hit Aceh in 2004, a remarkable example of local knowledge, '**Smong**' from Simeuleu Regency, was able to significantly minimize the number of deaths, with just seven fatalities from this area out of 200,000 across Aceh. The entire population understands the keyword of Smong as 'something bad' happens, for instance, an earthquake or tsunami. When the elderly shouted '**Smong**!' that day, all villages self-evacuated."*

However, on September 28, 2018, the local population faced a catastrophic tsunami that challenges the veracity of their local knowledge. Despite the inherent risks posed by such events, a considerable portion of the population hesitated to evacuate (Trias & Cook, 2022). Their faith in the proven reliability of local knowledge, which had safeguarded them in the past, played an important role in this reluctance. Moreover, there existed a prevailing skepticism towards official sources of information, which further deterred residents from leaving their homes (Trias & Cook, 2022). The failure of disaster management in Indonesia has been attributed to an overreliance on local knowledge and a lack of understanding of structural disaster management systems; local knowledge alone should not be the main factor for taking account of the people's safety (Juwitasari et al., 2022).

From a policy perspective, the Indonesian government has issued numerous policies and programs to enhance disaster preparedness and management in response to the threat posed by natural hazards. The main guideline for disaster management is Law No.24 of 2007, which is called 'Disaster Management'. Its purpose is to protect communities from natural disasters and encourage people to work together by planning and coordinating various aspects (Rustan & Firdaus, 2011). Regional governments have taken significant steps to develop disaster

management policies, strategies, and operations in alignment with Law No.24 of 2007, particularly through the enactment of Government Regulation No.21 of 2008, which addresses the implementation of disaster management (Pratama & Roza, 2019). However, when we reflect on several earthquakes that have struck Indonesia, like the 2018 Palu earthquake, it becomes evident that there are critical issues hindering policy effectiveness. One major challenge is communication, particularly the transmission, clarity, and consistency of information, all of which encounter technical obstacles and are hampered by inadequate means of communication (Achmad, 2023). Additionally, resources, notably infrastructure like shelters and heavy equipment, are insufficient (Anggriawan, 2019).

CHAPTER 2: LITERATURE REVIEW

2.1 Remote Sensing Techniques in Tsunami Analysis

Remote sensing, the science of obtaining information about objects or areas from a distance, typically from aircraft or satellites, has become a crucial tool in tsunami research and disaster management. This literature review examines the diverse applications of remote sensing techniques in tsunami analysis, highlighting advancements, methodologies, and key findings in this field.

Early Developments and Methodologies

The initial use of remote sensing in tsunami analysis focused on post-event damage assessment. Pioneering studies, like those following the 2004 Indian Ocean tsunami, utilized satellite imagery to map affected coastlines and assess the extent of inundation (Asoka Kumara, 2006). These early applications primarily used optical imagery and Synthetic Aperture Radar (SAR) data.

Advancements in Technology and Applications

Recent technological advancements have significantly broadened the scope of remote sensing in tsunami analysis. High-resolution satellite imagery, LiDAR (Light Detection and Ranging), and radar technologies have enabled more detailed and accurate assessments. For instance, Chiroiu et al. (2018) demonstrated the use of high-resolution satellite data for rapid damage assessment in coastal zones.

Tsunami Detection and Early Warning Systems

A critical application of remote sensing is in tsunami early warning systems. Studies like those by Tang et al. (2016) have explored the use of satellite altimetry data to detect sea-level

anomalies indicative of tsunamis. Similarly, SAR data, due to its ability to penetrate cloud cover and capture surface roughness, has been invaluable in detecting tsunami wavefronts and forecasting their impact (Liu et al., 2015).

Post-Event Damage Assessment and Recovery Planning

Remote sensing is extensively used for post-tsunami damage assessment. This involves mapping inundation areas, assessing structural damage, and evaluating the impact on natural resources. Studies by Gokon et al. (2017) have highlighted the use of remote sensing in understanding the extent of damage to aid effective recovery and rehabilitation efforts.

Environmental Impact Assessment

Remote sensing techniques are also employed to study the environmental impacts of tsunamis, such as changes in land cover, coastal erosion, and sedimentation. Research by Yamazaki et al. (2018) using multispectral imagery has provided insights into the long-term ecological effects of tsunamis on coastal environments.

Integration with GIS and Modelling Approaches

The integration of remote sensing data with Geographic Information System (GIS) platforms and modelling techniques has been a significant advancement. This integration allows for more comprehensive spatial analysis and modelling of tsunami risks and impacts. Studies by Andrade et al. (2019) illustrate how combining remote sensing data with GIS models can enhance tsunami hazard mapping and risk assessment.

Despite significant progress, challenges remain in remote sensing applications for tsunamis. These include limitations in spatial and temporal resolution, data availability, and the need for rapid data processing during emergency situations. Future research is likely to focus on

integrating real-time data processing, improving the accuracy of early warning systems, and enhancing the resolution of satellite data. Remote sensing has become an indispensable tool in tsunami analysis, offering valuable data for early warning, impact assessment, and recovery planning. As technology advances, its role in understanding and mitigating tsunami risks is likely to grow, providing more precise and timely information to safeguard vulnerable coastal communities.

2.2 Analytical Hierarchy Process

The Analytic Hierarchy Process (AHP), developed by Thoms L. Satty (2008), is a structured technique for organizing and analyzing complex decisions. It has been widely applied in various fields, including geography, where it aids in spatial decision-making processes. This literature review examines the application and effectiveness of AHP in geographical studies, highlighting key methodologies, applications and outcomes.

Methodological Framework

AHP in geography involves structuring a decision problem into a hierarchy, prioritizing each element, and synthesizing the results to determine the best option. Early applications, as discussed in Saaty's foundational works, focus on the method's theoretical underpinnings. Recent studies integrate AHP with Geographic Information Systems (GIS) for spatial decision-making (Malczewski, 2006; Banai, 1993), enhancing both spatial analysis and decision-making accuracy.

Applications

- Land Use Planning: AHP is widely used in land use planning. For instance, Feizizadeh and Blaschke (2013) demonstrated the use of AHP in evaluating land suitability for agricultural

purposes. Their study highlighted AHP's effectiveness in integrating various criteria, such as soil quality and accessibility, into land-use decision-making.

- Environmental Management: AHP has been instrumental in environmental management. Geneletti (2004) used AHP to assess the environmental impact of development projects, showing how AHP can balance ecological concerns with developmental needs.
- Urban Planning: In urban planning, AHP assists in infrastructure development and urban sprawl analysis. A study by Yeh and Huang (2009) employed AHP to prioritize urban development projects, showcasing its utility in managing complex urban planning scenarios.

Advantages and Limitations

The advantages of AHP in geography include its flexibility, its ability to handle both qualitative and quantitative data, and its facilitation of group decision-making (Saaty, 2008). However, the method is not without limitations. It can be subjective, as it relies heavily on the judgment of experts (Dyer, 1990). Additionally, the complexity of creating a comprehensive hierarchy can be a challenge in spatial analysis.

Recent Innovations

Recent advancements have focused on integrating AHP with other computational techniques. For instance, the combination of AHP and GIS, as seen in works by Malczewski (2006), provides a more robust tool for spatial analysis and decision-making. Further, the incorporation of AHP in participatory GIS frameworks has been explored to enhance community-based decision-making processes (Brown & Fagerholm, 2015).

AHP has proven to be a versatile and powerful tool in the field of geography. Its ability to decompose complex decisions into a structured hierarchy makes it particularly suitable for spatial decision-making. While it has certain limitations, such as potential subjectivity and complexity, its integration with GIS and other computational methods has expanded its utility. Future research may focus on addressing its limitations and exploring its application in emerging geographical challenges, such as climate change adaptation and sustainable development planning.

CHAPTER 3: RESEARCH QUESTIONS

Studies has shown that the financial impact of natural disasters is significant and rising (Kreimer, 2001; Kellenberg et al., 2008; Keerthiratne et al., 2017; Chang & Zhang, 2020). For instance, in the United States, the cost of recovery from climate change-related natural disasters has exceed $2 trillion since 1980 (National Oceanic and Atmospheric Administration, 2021). A particular study from the Disaster Medicine Fellowship at Beth Israel Deaconess Medical Center highlighted that there has been a steady increase in the frequency and severity of billion-dollar disasters over the years, which has led to higher recovery costs (Bhola et al., 2023). Additionally, investments in disaster risk mitigation can be economically beneficial; research suggests that every dollar spent on mitigation can save a substantial amount in post-disaster rebuilding efforts (Bhola et al., 2023). The costs associated with natural disaster management in Palu, which include research, disaster preparedness, and other aspects, has been substantial (Samad et al., 2021). In the aftermath of 2018 earthquake and tsunami, the region faced significant challenges. While specific financial figures for research and disaster preparedness activities in Palu are not readily available, the overall impact of losses was estimated to be Rp. 2.89 trillion, with damage costs amounting to Rp. 15.58 trillion due to the disaster (Damarjati et al., 2018).

This study aims to use easy, handy, and low-cost Remote Sensing and GIS techniques to quickly identify tsunami-affected zones and to develop a simple model for detecting tsunami-vulnerable areas in Palu. This is to enhance future disaster readiness. In doing so, there are two major questions to answer:

- How can Remote Sensing techniques be applied to accurately map and assess the extent of areas affected by the 2018 Sulawesi Earthquake and Tsunami in Palu?

The answer to this question should be a low-cost methodology using satellite imagery from open sources that can be simple and quick with the potential to be implemented in an early warning system or post-disaster for disaster management.

- What is the relationship between geospatial variables such as elevation, slope, coastal proximity, and land use in defining the tsunami vulnerability in Palu, and how do these variables correlate with the observed patterns of damage resulting from the 2018 Sulawesi earthquake and tsunami?

  By using easy to calculate derivatives of a DEM (e.g. slope, elevation) I am attempting to come up with a quick estimate of tsunami vulnerability using only a handful of metrics.

The tsunami signature on the ground varies from event to event and location to location but with respect to Palu, large flooding, debris, ground erosion and scouring and structural damage were some of the prominent ways the tsunami impacted Indonesia. The Remote sensing techniques used in this thesis are meant to capture the imprint of tsunamis in the post-disaster landscape. The remote sensing analysis is capturing all these through a combination of common tools such as indices, color composites, classification and threshold analysis. For example, Normalized Difference Vegetation Index (NDVI) is used to estimate the vegetation density but in a post-tsunami environment, NDVI should be able to determine extent of vegetation erosion and increased soil moisture. One hypothesis is that the density of vegetation in the study area will decrease following the tsunami, as indicated by a decline in NDVI values, while water and soil indices are expected to increase. NDVI is supplemented by Normalized Difference Water Index

(NDWI), and Normalized Difference Soil Index (NDSI) as indicators to identify water and soil changes, therefore, acting as a proxy of the tsunami impact on the ground.

Previous research has verified that it is possible to identify tsunami inundated areas by observing changes in spectral indices. Specifically, Yamazaki et al. (2005) carried out a field survey in Southern Thailand to examine areas severely affected by the Banda Aceh 2004 Boxing Day tsunami (e.g. Paris et al., (2009); Lavigne et al., (2009); Borrero et al., (2005)), using GPS cameras and a handheld spectrometer. Three conditions of vegetation were measured: healthy (replanted), seriously affected (yellow), and dead. There were clear differences in the reflectance curves among these three conditions, with healthy plants showing a rapid increase in reflectance between the visible red (R) and near-infrared (NIR) bands. This characteristic was reduced in the unhealthy plants and absent in the dead plants (Yamazaki et al., 2005). These significant changes in vegetation reflectance can be used to assess the effects of the tsunami.

Regarding research question 2, geospatial variables such as elevation, slope, coastal proximity and land use are identified as key factors in developing a simple GIS model to detect tsunami-vulnerable areas in Palu. This model utilizes the Analytical Hierarchy Process (AHP) method to systematically evaluate and prioritize these variables for effective disaster preparedness planning.

CHAPTER 4: MATERIALS & METHODS

4.1 Study Area

This study was carried out in the Palu city region (Figure 1). Palu is the capital and largest city of Central Sulawesi in Indonesia, with the boundary between 0°39'S to 0°56'S and 119°45'E to 120°1'E), and with an area of 395.06 km^2 (Palu, 2022). According to the 2020 Indonesian census (2021), Palu had a population of 373,218, making it the third-most populous city on the island after Makassar and Manado. Palu is situated on the Palu-Koro Fault and is frequently struck by earthquakes, such as the 2018 Sulawesi earthquake. According to Indonesia's National Disaster Management Agency [4], the earthquake-triggered secondary natural disasters, including soil liquefaction, landslides, and tsunamis, significantly affected Palu. For example, the 2018 earthquake caused 'the largest natural soil liquefaction phenomenon in the world' (Indonesia CNN, 2018).

[4] Please find more information through Indonesia's National Disaster Management Agency Website: https://www.preventionweb.net/organization/national-agency-disaster-management-badan-nasional-penanggulangan-bencana\

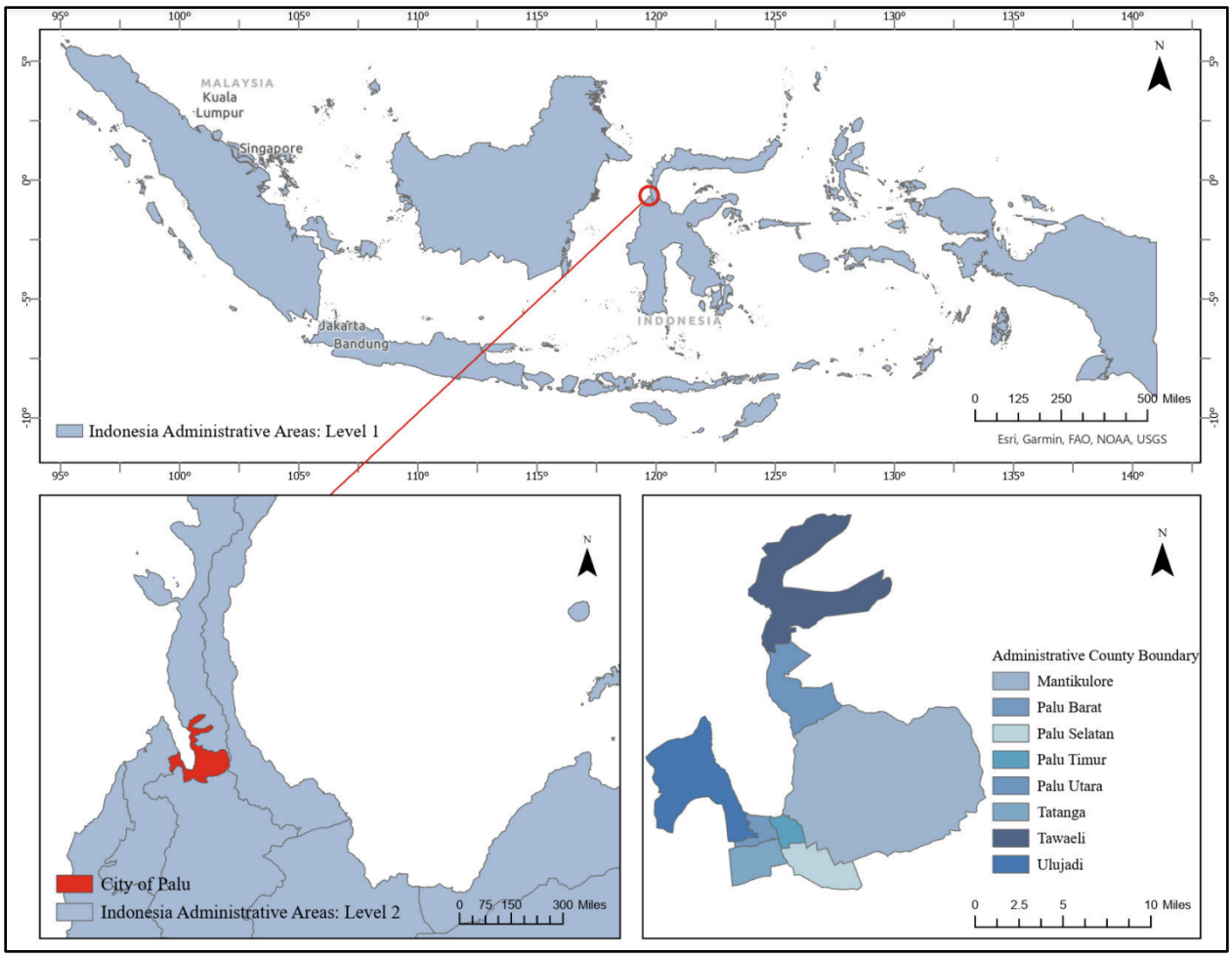


Figure 1 Study Area the City of Palu. Data Source: AHA – Indonesia Subnational Administrative Boundary

4.2 Data

4.2.1 Remote Sensing Imagery

Our primary data is Sentinel-2 imagery. Sentinel-2 is a European Space Agency (ESA) satellite mission consisting of two identical satellites, Sentinel-2A and Sentinel-2B, launched in 2015 and 2017, respectively (European Space Agency, n.d.). The Sentinel-2 satellites are equipped with a high-resolution multispectral imaging instrument, capable of capturing images of the Earth's surface with a spatial resolution of up to 10 meters (European Space Agency, n.d.). The instrument can collect data in 13 spectral bands, ranging from the visible to the near-infrared, which can be used for a variety of applications, including land use and land cover mapping, vegetation monitoring, and disaster response (European Space Agency, n.d.). To provide a better understanding of the before and aftereffects of the tsunami, two images were captured at different times. The first image was taken on September 27, 2018, serving as a pre-tsunami depiction. The second image, captured on October 2, 2018, was taken as a post-tsunami representation.

Table 2 Sentinel-2 Imagery Description Table [5]

	Satellite & Mission ID	Product Level	Spatial Resolution	Band Number	Production Baseline	Orbit Number	Acquisition Sensing Time
Pre-tsunami	Sentinel-2 S2B	Level-1C	10m	Band 2 Band 3 Band 4 Band 8	N0206	R103	09/27/2018
	Sentinel-2 S2B	Level-1C	20m	Band 5 Band 6 Band 7 Band 8A Band 11	N0206	R103	09/27/2018

[5] Data Source: European Space Agency's (ESA) Copernicus Programme. https://scihub.copernicus.eu/

				Band 12			
	Sentinel-2 S2B	Level-1C	60m	Band 1 Band 9 Band 10	N0206	R103	09/27/2018
	Sentinel-2 S2A	Level-1C	10m	Band 2 Band 3 Band 4 Band 8	N0206	R103	10/02/2018
Post-tsunami	Sentinel-2 S2A	Level-1C	20m	Band 5 Band 6 Band 7 Band 8A Band 11 Band 12	N0206	R103	10/02/2018
	Sentinel-2 S2A	Level-1C	60m	Band 1 Band 9 Band 10	N0206	R103	10/02/2018

Another Remote Sensing dataset included in this study is Maxar WorldView-3 Imagery. Maxar Technologies is a leading space technology and intelligence company that operates a lot of commercial imaging satellites. These satellites are capable of capturing high-resolution imagery of the Earth and are used for a wide range of applications such as environmental monitoring, urban planning and disaster management. Maxar Technologies provides free satellite imagery for disaster response through their Open Data Program [6]. This program releases high-quality geospatial data to aid organization during major crisis events. Maxar's Open Data Program has been activated for various events, including natural disasters like earthquakes and hurricanes, providing a crucial response for disaster management and relief efforts.

[6] Maxar Open Data Program: https://www.maxar.com/open-data

Table 3 Maxar WorldView Imagery Description Table [7]

	Satellite	Band Number	Spatial Resolution	Acquisition Sensing Time
Pre-tsunami	WorldView-3	1 Panchromatic band (450 - 800 nm)	0.31m	08/17/2018
	WorldView-3	8 Visible Near Infrared (VNIR) bands	1.24 meters at nadir	08/17/2018
	WorldView-3	8 Shortwave Infrared (SWIR) bands	3.70 meters at nadir	08/17/2018
	WorldView-3	12 CAVIS (Clouds, Aerosols, Vapors, Ice, & Snow) bands	30 meters at nadir	08/17/2018
Post-tsunami	WorldView-3	1 Panchromatic band (450 - 800 nm)	0.31m	10/02/2018
	WorldView-3	8 Visible Near Infrared (VNIR) bands	1.24 meters at nadir	10/02/2018
	WorldView-3	8 Shortwave Infrared (SWIR) bands	3.70 meters at nadir	10/02/2018
	WorldView-3	12 CAVIS (Clouds, Aerosols, Vapors, Ice, & Snow) bands	30 meters at nadir	10/02/2018

[7] Data Source: MAXAR. https://www.maxar.com/

4.2.2 Geographic Data

Table 4 Topographic Elevation Data

Topographic Elevation Data	
Data Product	Shuttle Radar Topography Mission (SRTM)
Product Level	1 Arc-Second Global
Digital Object Identifier (DOI) number	/10.5066/F7PR7TFT
Spatial Resolution	1 arc-second for global coverage (~30 meters)
Raster Size	1-degree tiles
C-band Wavelength	5.6cm
Acquisition Sensing Time	2014-09-23 00:00:00-05

Table 5 Land Use Data

Land Use Data	
Data Product	Sentinel-2 10m Land Use/land Cover
Product Level	Sentinel-2 L2A
Sensors	Multispectral Instrument (MSI)
Spatial Resolution/Cell Size	10m
Type	Thematic
Attribution	Esri, Impact Observatory, and Microsoft
Acquisition Sensing Time	2018

Table 6 Indonesia Administrative Boundary Data

Indonesia Administrative Boundary Data	
Source	Badan Pusat Statistik (BPS - Statistics Indonesia)
Contributors	OCHA Regional Office for Asia and the Pacific (ROAP)
Reference Period	April 08, 2020-November 24, 2023

Type /File Format	Vector / Shapefile
Indonesia Administrative Level	Level 0: country – negara Level 1: province – provinsi Level 2: city, district, regency - kota, kabupaten Level 3: sub-district - kecamatan, distrik Level 4: village - desa, kelurahan, kampung, nagari, pekon or gampong

4.3 Methodology

4.3.1 Remote Sensing Workflow

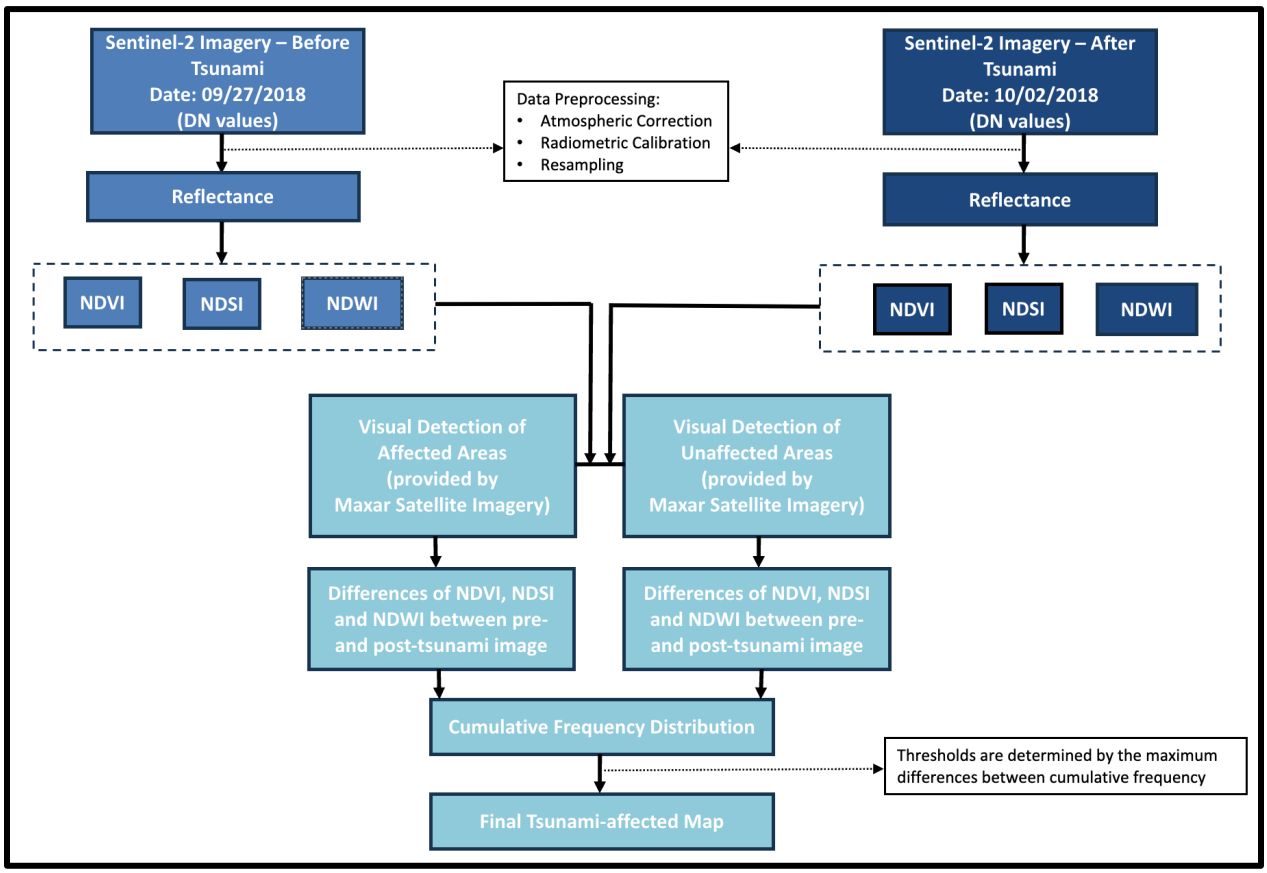


Figure 2 Remote Sensing Workflow – Research Question 1

The workflow in Figure 2 details the procedure for using remote sensing data to determine tsunami-impacted areas. It involves the following steps:

- Acquisition of Sentinel-2 imagery for the periods before and after the tsunami.
- Data preprocessing, which includes atmospheric correction, radiometric calibration, and resampling to convert the raw Digital Number (DN) values into reflectance values.

- Calculation of NDVI, NDSI, and NDWI indices from the reflectance data to identify different land and water features.
- Visual detection using Maxar Satellite Imagery to discern areas affected and unaffected by the tsunami.
- Analysis of the differences in the indices pre- and post-tsunami to identify changes in vegetation, soil, and water features.
- Application of a cumulative frequency distribution to determine the thresholds for the differences in indices, which helps to classify the areas based on the level of impact.
- The output is a final map that clearly delineates the areas affected by the tsunami, providing a valuable tool for disaster response and assessment.

4.3.2 Index Formulas

To quantify vegetation, the Normalized Difference Vegetation Index (NDVI) uses a method of measuring the contrast between near-infrared light (which vegetation reflects powerfully) and red light (which vegetation absorbs). This technique assists in evaluating the amount and health of plant growth, with elevated NDVI values indicating more abundant vegetation, with open- water features effectively suppressed (Mcfeeters, 1996). The NDVI is calculated as:

$$NDVI = Index\ (NIR, RED) = \frac{(NIR - RED)}{(NIR + RED)}$$

For Sentinel-2, the vegetation index is calculated as:

$$NDVI\ = \ Index\ (B8, B4)\ = \frac{(B8 - B4)}{(B8 + B4)}$$

Where Red and NIR are the reflectance of red and near-infrared bands, respectively. The NDVI formula takes these differences into account and generates a value ranging from -1 to +1, where higher values indicate healthier and more abundant vegetation. If the NDVI equation were inverted and the green band were employed, the results would likewise be inverted, with vegetation being suppressed and open-water features enhanced (Mcfeeters, 1996). The equation for normalized difference water index (NDWI) is calculated as follows:

$$NDWI = Index\,(GREEN, NIR) = \frac{(GREEN - NIR)}{(GREEN + NIR)}$$

For Sentinel-2, the water index is calculated as:

$$NDWI = Index\,(B3, B8) = \frac{(B3 - B8)}{(B3 + B8)}$$

Where Green and NIR are the reflectance of green and near-infrared bands, respectively. The outcomes from this equation are water features that have positive values while soil and terrestrial vegetation have zero or negative values. The equation for normalized difference soil index (NDSI) (Kouchi et al., 2007) is:

$$NDSI = Index\,(RED, BLUE) = \frac{(RED - BLUE)}{(RED + BLUE)}$$

For Sentinel-2, the soil index is calculated as:

$$NDSI = Index\,(B4, B2) = \frac{(B4 - B2)}{(B4 + B2)}$$

4.3.3 Tsunami Vulnerability Model Workflow

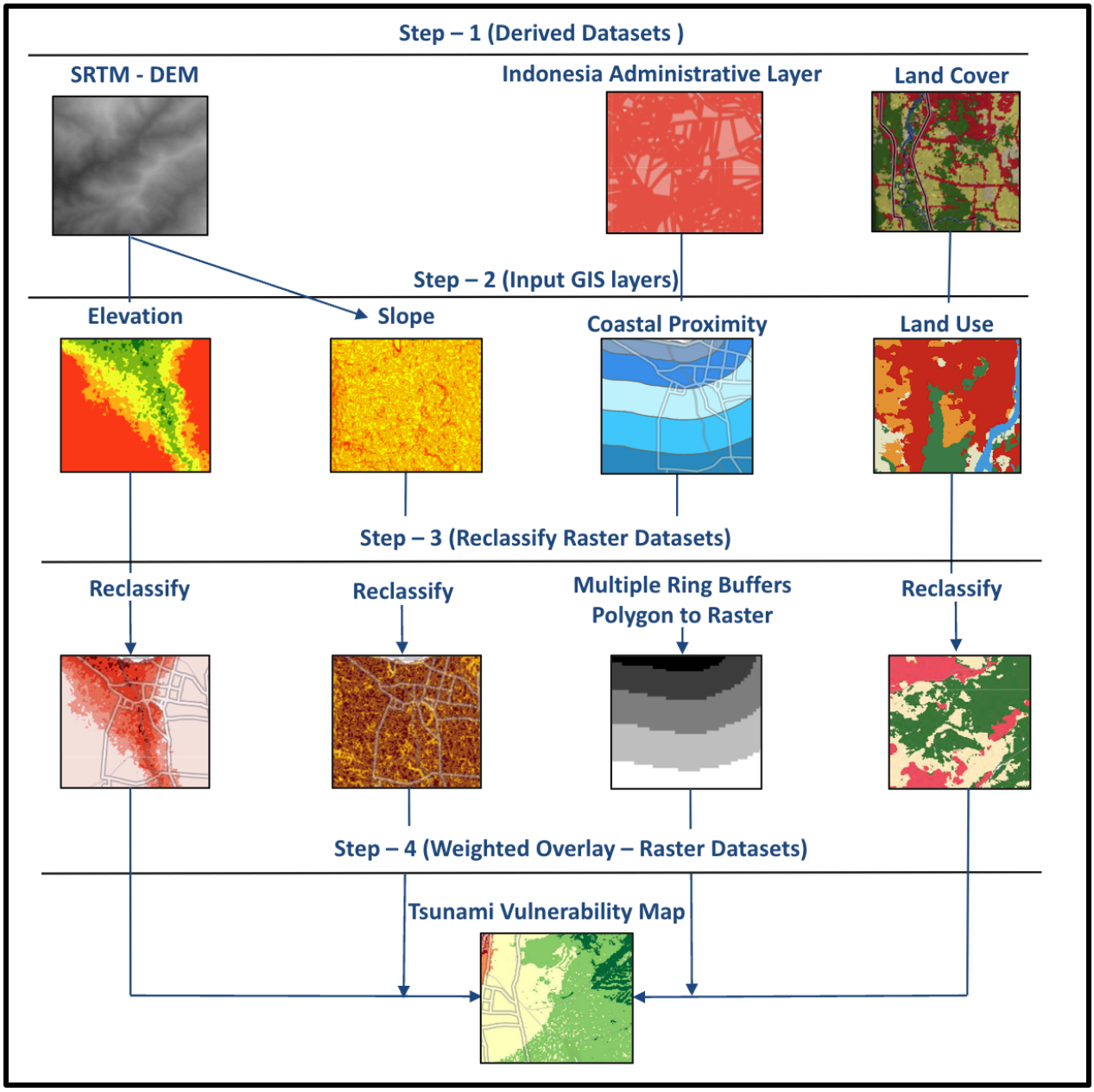


Figure 3 Main methodology steps followed for the tsunami vulnerability mapping based on different factors – Research Question 2

The workflow depicted in the Figure 3 is a structured approach to constructing a tsunami vulnerability map for Palu, taking into account various geospatial factors. Initially, derived datasets such as SRTM – DEM provide the foundational elevation data, supplemented by

administrative and land cover information to form a comprehensive base. These datasets are processed to create GIS layers that reflect elevation, slope, coastal proximity, and land use – each representing crucial elements that influence susceptibility to tsunamis.

Subsequently, each of these layers undergoes a reclassification process, standardizing the data into a more manageable and relevant form for analysis. The coastal proximity data, in particular, is further processed through the application of multiple buffers to demarcate distances from the coastlines, which is then translated into a raster format to align with the other factors.

The culmination of the workflow is a weighted overlay analysis where the reclassified raster datasets are synthesized. This integration is weighted, meaning each factor's relative importance in determining vulnerability is quantified and applied during the overlay process. The result is a comprehensive tsunami vulnerability map that identifies areas with varying risk levels, providing an essential tool for disaster preparedness and risk mitigation strategies.

CHAPTER 5: REMOTE SENSING ANALYSIS

5.1 False Color Composite

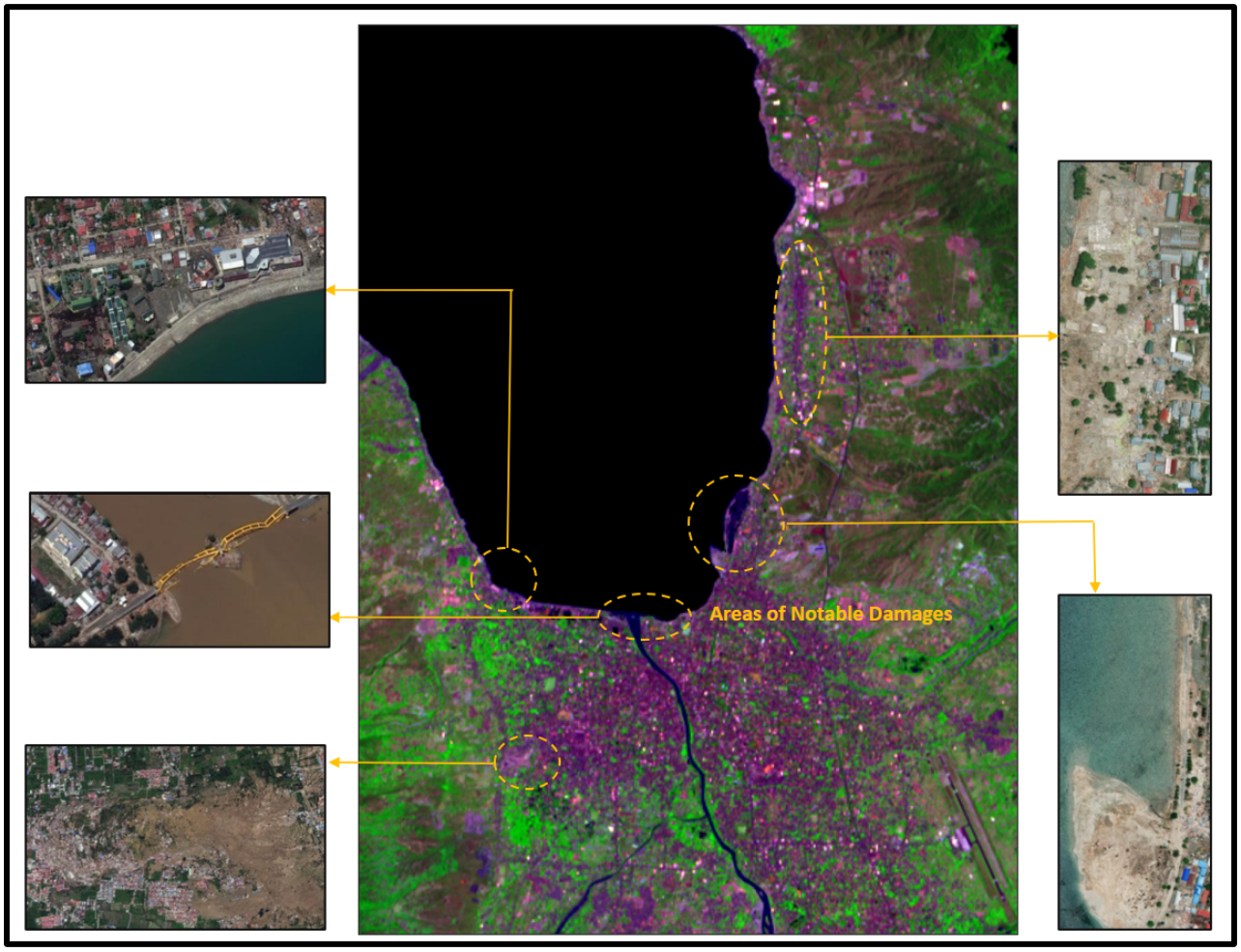


Figure 4 False Color Composite after tsunami (10/02/2018) (SWIR, VNIR and RED as RGB bands)

The image is a false color composite satellite image taken after a tsunami event on October 2, 2018. A false color composite uses non-visible bands of the electromagnetic spectrum and maps them to visible colors to highlight features that are not easily discerned in true-color imagery. Here, Short-Wave Infrared (SWIR), Visible Near Infrared (VNIR), and Red bands are assigned to the RGB (Red, Green, Blue) color channels respectively. In false color composites,

vegetation often appears in shades of green, while water bodies can appear in various colors depending on the particular band combination used (dark blue in Figure 4). Urban areas or bare ground typically appear in shades of purple, pink, grey, or brown (purple in Figure 4).

5.2 Computation of Indices

5.2.1 Normalized Difference Vegetation Index

Figure 5 shows NDVI values for pre- and post-tsunami imagery, which already reclassification based on the criteria NDVI classification developed by Al-Doski et al. (2013). The NDVI is a measure of vegetation health, with higher values indicating denser, healthier vegetation. In Figure 5, three classes are depicted: water, snow, and clouds represented with values from -1 to 0, barren land, built-up areas, and rock with values from 0 to 0.2, and vegetation from 0.2 to 1. The comparison shows little change in the water, snow, and cloud class, while there is an apparent increase in barren land, suggesting vegetation loss and soil exposure due to the tsunami. This significant alteration within a five-day interval suggests the devastating impact of the tsunami on the land surface.

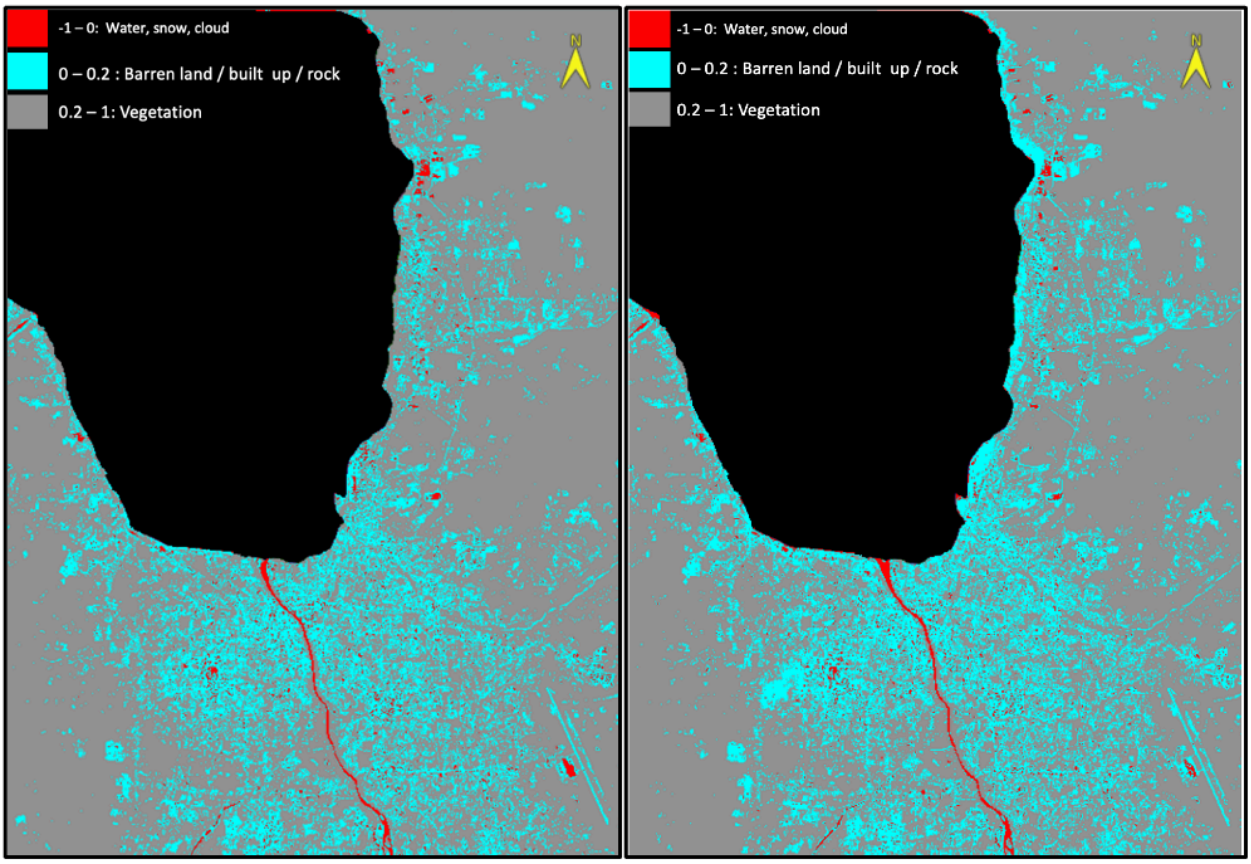


Figure 5 Reclassification NDVI for pre-tsunami (09/27/2018) (left) and post-tsunami imagery (10/02/2018) (right)

Table 7 NDVI Value Calculation for Pre- and Post-tsunami Imagery

	Min	Max	Mean	StdDev
NDVI: Pre-tsunami Imagery (09/27/2018)	-0.3.2267	0.951316	**0.366168**	0.200242
NDVI: Post-tsunami Imagery (10/02/2018)	-0.417379	0.884233	**0.342750**	0.190555

Table 7 presents NDVI calculations before and after a tsunami event. Pre-tsunami imagery had a minimum NDVI of -0.32267 and a maximum of 0.951316, with a mean value of 0.366168 and a standard deviation of 0.200242. Post-tsunami imagery shows a decrease in both maximum and mean NDVI values, with the minimum NDVI dropping to -0.417379, the maximum to 0.884233, and the mean to 0.342750. The standard deviation after the tsunami is 0.190555. This

indicates a general reduction in vegetation health immediately following the tsunami.

5.2.2 Normalized Difference Water Index

Figure 6 depicts the Normalized Difference Water Index (NDWI) maps side by side for a region before (left) and after (right) a tsunami. The NDWI helps identify water features, which are mapped within a value range from 0 to 1. Areas classified as non-water features have values of -1 to 0. The pre-tsunami map shows the distribution of water bodies on September 27, 2018, while the post-tsunami map shows how these distributions have changed by October 2, 2018, likely due to the inundation caused by the tsunami. The maps provide visual evidence of the changes in water extent as a result of the disaster.

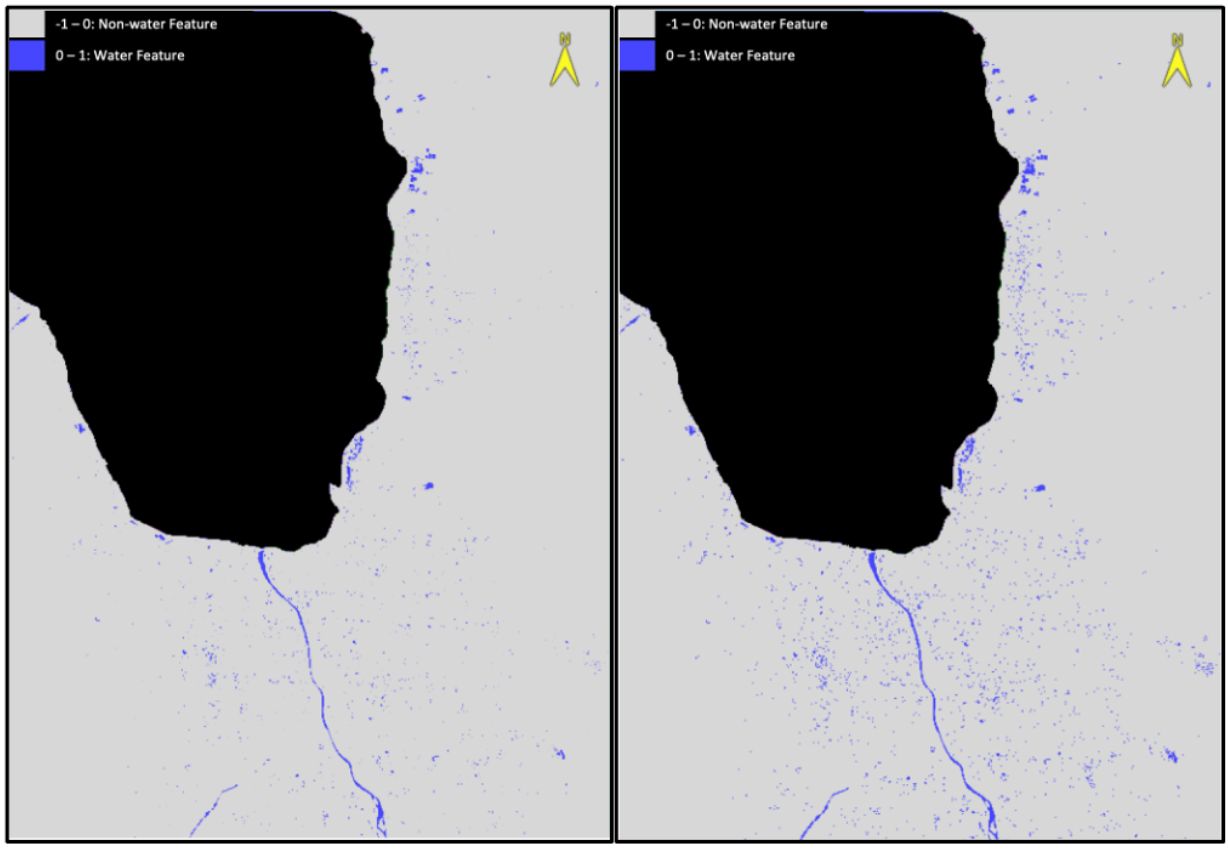


Figure 6 Reclassification NDWI for pre-tsunami (09/27/2018) (left) and post-tsunami imagery (10/02/2018) (right)

Table 8 NDWI Value Calculation for Pre- and Post-tsunami Imagery

	Min	Max	Mean	StdDev
NDWI: Pre-tsunami Imagery (09/27/2018)	-0.95269	0.500502	**-0.382440**	0.170663
NDVI: Post-tsunami Imagery (10/02/2018)	-0.999283	0.535354	**-0.3667338**	0.163924

Table 8 presents the NDWI values before and after the tsunami, with the post-tsunami mean NDWI slightly higher than the pre-tsunami mean, indicating a marginal increase in water content. However, the difference is small. A clearer understanding of the changes is obtained by examining Figure 6, which likely provides a visual representation of the distribution and extent of water features that more distinctly highlights the impact of the tsunami.

5.2.3 Normalized Difference Soil Index

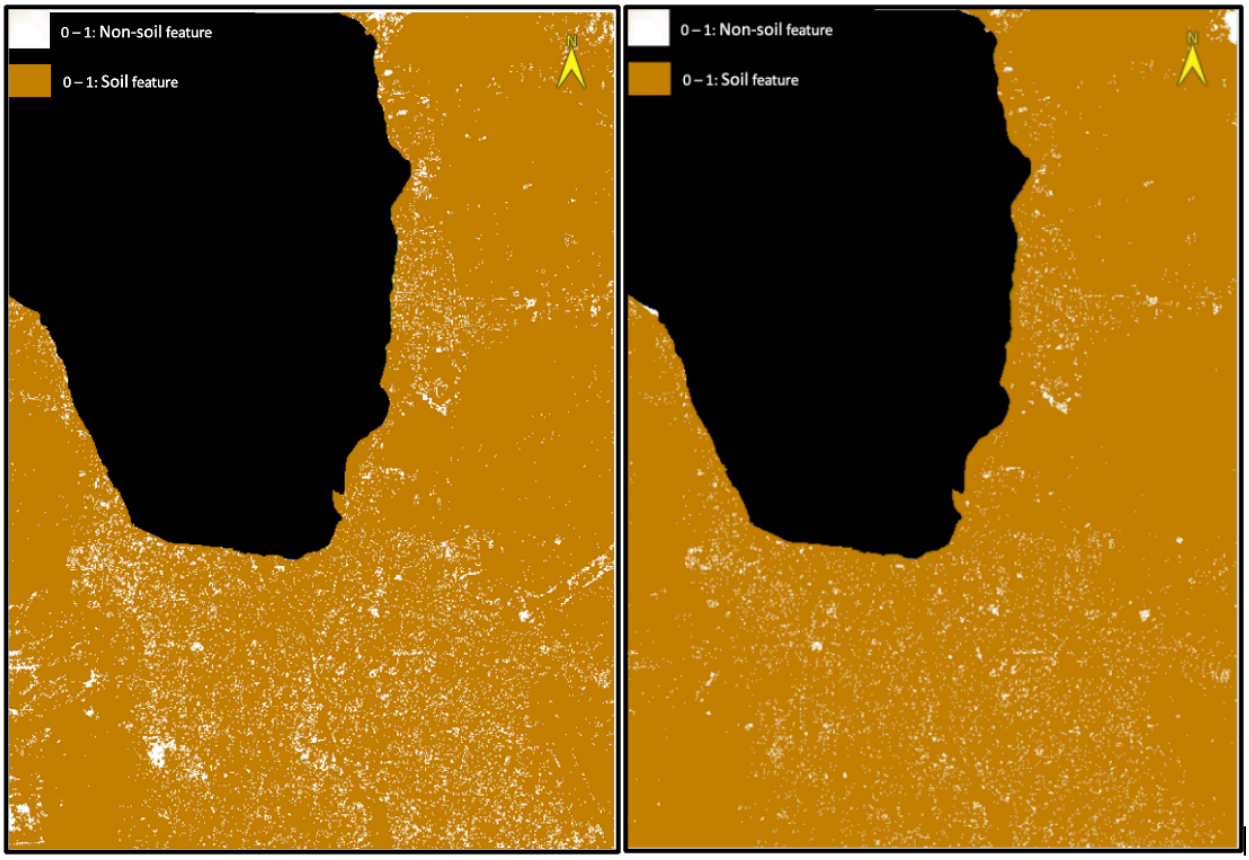


Figure 7 Reclassification NDSI for pre-tsunami (09/27/2018) (left) and post-tsunami imagery (10/02/2018) (right)

As shown in Figure 7, the NDSI helps identify soil surface changes, and in this instance, a clear increase in soil features (in yellow) is visible in the post-tsunami image to the right. This suggests that the tsunami's impact may have resulted in the removal of vegetation or other cover, revealing more of the soil surface underneath.

Table 9 NDSI Value Calculation for Pre- and Post-tsunami Imagery

	Min	Max	Mean	StdDev
NDSI: Pre-tsunami Imagery (09/27/2018)	-0.661308	0.658560	**0.113160**	0.081158

NDSI: Post-tsunami Imagery (10/02/2018)	-0.569260	0.998762	**0.138013**	0.076420

Table 9 provides statistical data for the Normalized Difference Soil Index (NDSI) from imagery captured before and after a tsunami. The NDSI is used to differentiate between soil and non-soil surface features. The post-tsunami imagery shows an increase in both the maximum NDSI value and the mean NDSI value, indicating a greater presence or exposure of soil features after the event. This can be attributed to the disturbance caused by the tsunami, which may have cleared away vegetation or other surface materials, exposing the soil underneath. The standard deviation in the post-tsunami data is slightly lower than in the pre-tsunami data, suggesting less variability in soil exposure after the tsunami.

5.3 Threshold Analysis

In order to obtain more precise threshold values, we concentrated on a smaller research area located in the northeast part of Palu that was highly affected by the tsunami and had a clear boundary between the impacted and unaffected areas. By narrowing down the study area, we can conduct more rigorous analysis to gain a better understanding of the disaster's extent. This approach will allow us to provide more precise data for threshold analysis and mapping of the tsunami-affected regions, thereby increasing the accuracy of the results.

The NDVI, NDSI, and NDWI were calculated based on the formulas presented in Chapter 3. Typically, higher NDVI values indicate greater vegetation coverage, while higher NDSI and NDWI values indicate more soil moisture and water bodies, respectively. The significant changes of NDVI, NDSI and NDWI values in tsunami-affected areas are seen in Figure 8. As shown in Figure 8, NDVI decreases, and NSDI and NDWI increase in the tsunami-affected areas. These observations are based on the effects of the tsunami, which caused vegetation to wash away or become dead/weakened, exposed the soil, and increased soil moisture. Differences in the indices between areas affected and unaffected by the tsunami are readily apparent, and these disparities can serve as reliable indicators of tsunami inundation.

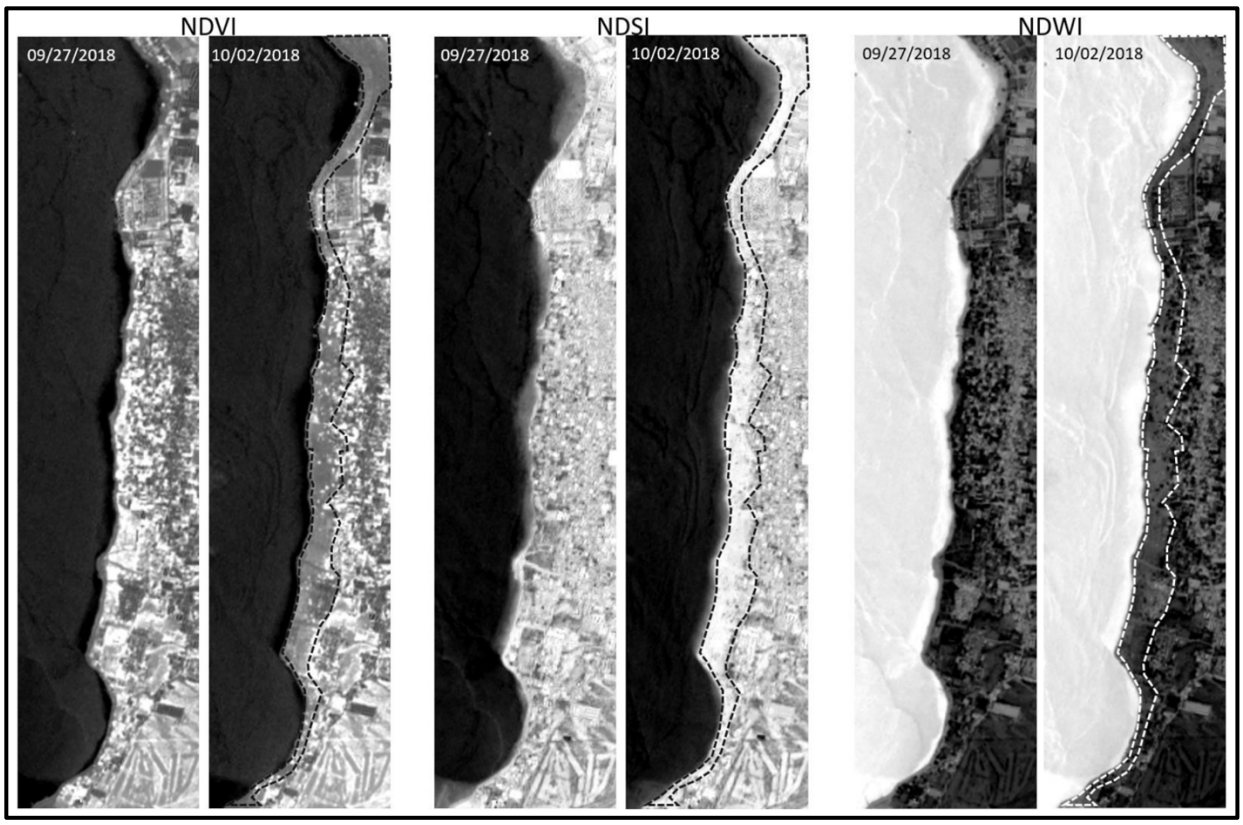


Figure 8 Computed NDVI, NDSI, and NDWI for pre-tsunami (09/27/2018) and post-tsunami (10/02/2018) in small areas of Palu

Research indicates two methodologies for setting threshold values to assess tsunami impact: using solely post-tsunami imagery or comparing both pre- and post-tsunami images (Kouchi et al., 2007). The first approach is viable when pre-event images are unavailable. However, juxtaposing images from before and after an event typically yields a more accurate assessment (Kouchi et al., 2007). This study employs the comparative method for a spatial analysis of the tsunami's effects and to establish more reliable threshold values.

Using Both the pre-tsunami and post-tsunami images:

As previously mentioned, Figure 8 highlights significant changes in NDVI, NDSI, and NDWI values in areas affected by the tsunami. It is possible to identify areas affected by the tsunami by computing the difference between the indexes obtained from pre-tsunami and post-tsunami

images. Recent advancements in remote sensing and related technologies have made it increasingly feasible to acquire both pre-event and post-event images. As a result, using such imagery to detect changes between the two can be an effective tool in identifying areas affected by natural disasters such as tsunamis.

The image was taken on September 27, 2018, serving as a pre-tsunami depiction, while the one captured on October 2, 2018, was taken as a post-tsunami representation. To further analyze the data, the distribution of index differences between affected and unaffected areas was calculated. The resulting cumulative frequency distribution of the time difference for NDVI, NDSI, and NDWI in both affected and unaffected areas is displayed in Figure 6. By identifying the maximum difference between their cumulative frequency distributions, it is feasible to establish a threshold value that can effectively distinguish the two classes. Utilizing this approach, the calculated thresholds for NDVI, NDSI, and NDWI were found to be -0.2, 0, and 0.04, respectively.

In summary, based on pre-tsunami and post-tsunami images, pixels with an NDVI (-0.2) value below the calculated threshold and NDSI (0) and NDWI values (0.04) exceeding the determined thresholds are classified as tsunami-affected areas.

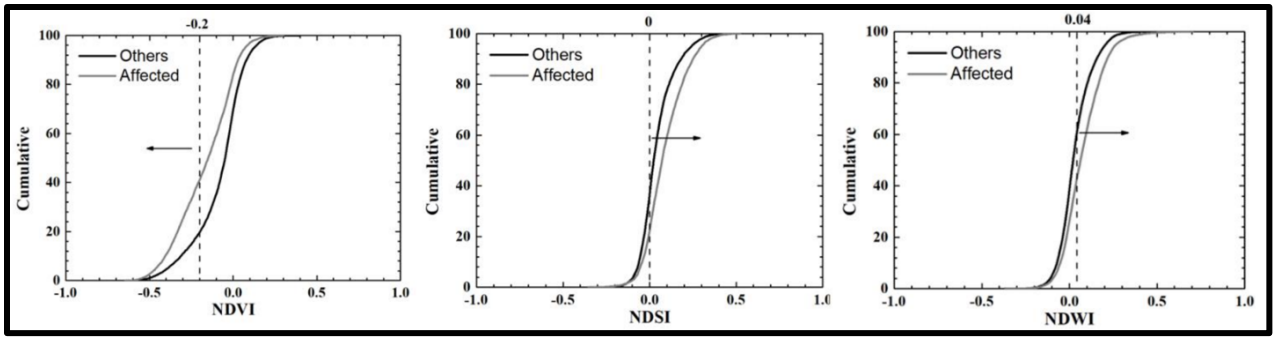


Figure 9 Cumulative Frequency Distribution of the differences of NDVI, NDSI and NDWI

5.4 Tsunami-Affected Areas Based on Thresholds of NDVI, NDSI, and NDWI

After obtaining the thresholds for the indices, we proceeded to apply these values to research areas, as illustrated in Figure 10. As we described in Section 4.3, pixels with an NDVI value below the calculated threshold (<-0.2) and NDSI and NDWI values exceeding the determined thresholds (>0 and >0.04) are classified as tsunami-affected areas. Illustrated in Figure 10, the entire city was impacted by the tsunami, with the tsunami-affected areas primarily concentrated along the coastal regions of Palu. Furthermore, it is important to note that the Balaroa city, located in the southwest part of Palu, was also affected by a soil liquefaction after the earthquake and subsequently buried.

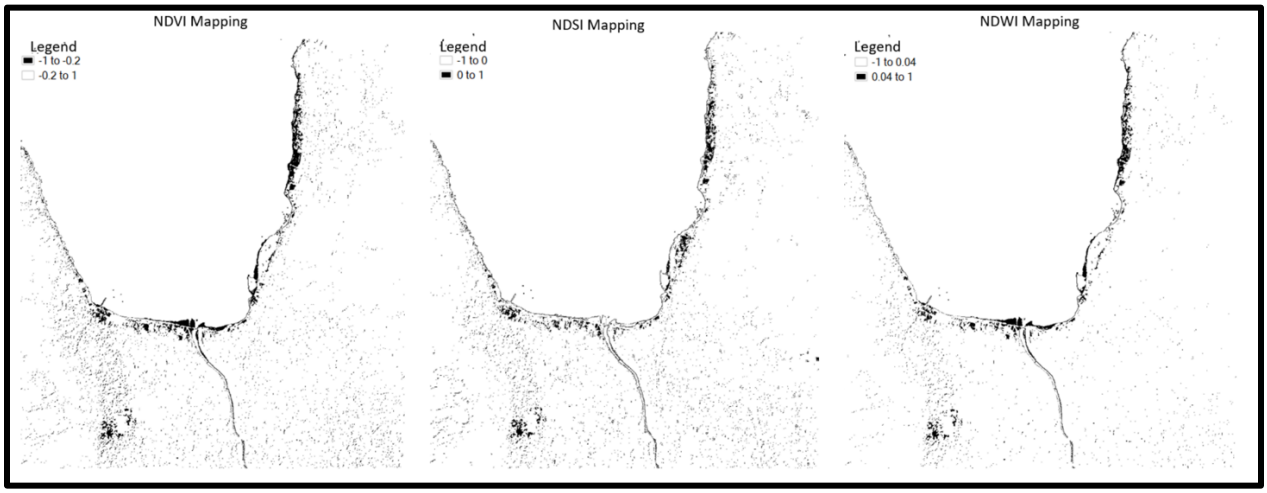


Figure 10 Mapping NDVI, NDSI and NDWI based on the threshold values

To derive the final tsunami-affected areas image, the decision tree classification approach is employed using dNDVI, dNDSI and dNDWI values obtained from pre- and post-events indices after applying thresholds based on the cumulative frequency distribution, as detailed in Section 5.3. Pixels with values below the NDVI threshold (-0.2), and above the NDSI (0) and NDWI (0.04) thresholds, are classified as tsunami-affected areas. The decision tree leverages these indices to

discern between water, soil, and vegetation changes due to the tsunami. Figure 11 visualizes the result, marking tsunami-impacted regions, which are notably more extensive along the coastal areas. This method is particularly effective as it combines multiple indices to enhance the accuracy of the classification, especially in complex environments where a single index may not be sufficient.



Figure 11 Final Tsunami Inundation Map based on Decision Tree

CHAPTER 6: GEOSPATIAL DATA ANALYSIS

6.1 Topographic Elevation Mapping

The Shuttle Radar Topography Mission (SRTM) Digital Elevation Model (DEM) was utilized to acquire the topographic elevations of the study areas. Following Lidia's (1963) classification of tsunami run-up heights along the coast, the topographic elevations were categorized into five distinct classes. The classification into five classes is outlined in Table 7. Additionally, Figure 9 presents the tsunami vulnerability map, which has been constructed based on topographic elevation data.

Table 10 Tsunami Vulnerability based on Topographic Elevation (Lidia, 1963)

Elevation (m)	Tsunami Vulnerability
<5	High
5 – 10	Slightly High
10 – 15	Medium
15 – 20	Slightly Low
>20	Low

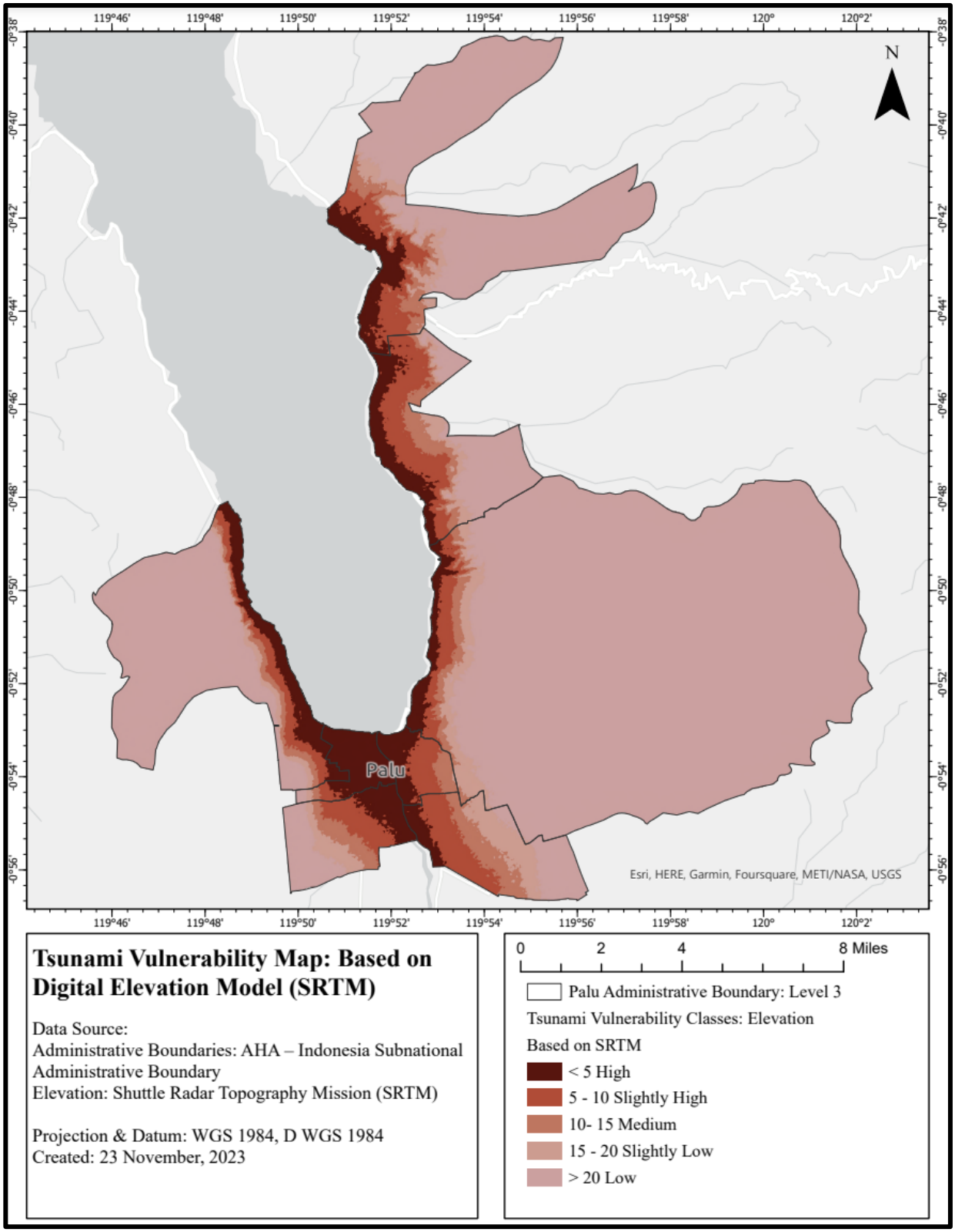


Figure 12 Tsunami Vulnerability Map based on Topographic Elevation

6.2 Topographic Slope Mapping

The slope identifies the steepness at each cell of a raster surface. The lower the slope value, the flatter the terrain; the higher the slope value, the steeper he terrain. The Planar method was used to calculated slope, and the slope is measured as the maximum rate of change in value from a cell to its immediate neighbors. The calculation is performed on a projected flat plane using a 2D Cartesian coordinate system. The slope value is calculated using a third-order finite difference estimator proposed by Horn (1981). The slope is computed as the rate of change (delta) of the surface in the horizontal (dz/dx) and vertical (dz/dy) directions from the center cell to each adjacent cell (Burrough & McDonnell, 1998). The basic algorithm used to calculate the slope is as follows:

$$slope_{radians} = ATAN\left(\sqrt{\left(\left[\frac{dz}{dx}\right]^2 + \left[\frac{dz}{dy}\right]^2\right)}\right)$$

Slope was reclassified using the criteria show in Table 8, and tsunami vulnerability based on slope is shown in Figure 10.

Table 11 Tsunami Vulnerability based on Topographic Slope (Van Zuidam, 1983)

Slope (%)	Tsunami Vulnerability
0 – 2	High
2 – 6	Slightly High
6 – 13	Medium
13 – 20	Slightly Low
> 20	Low

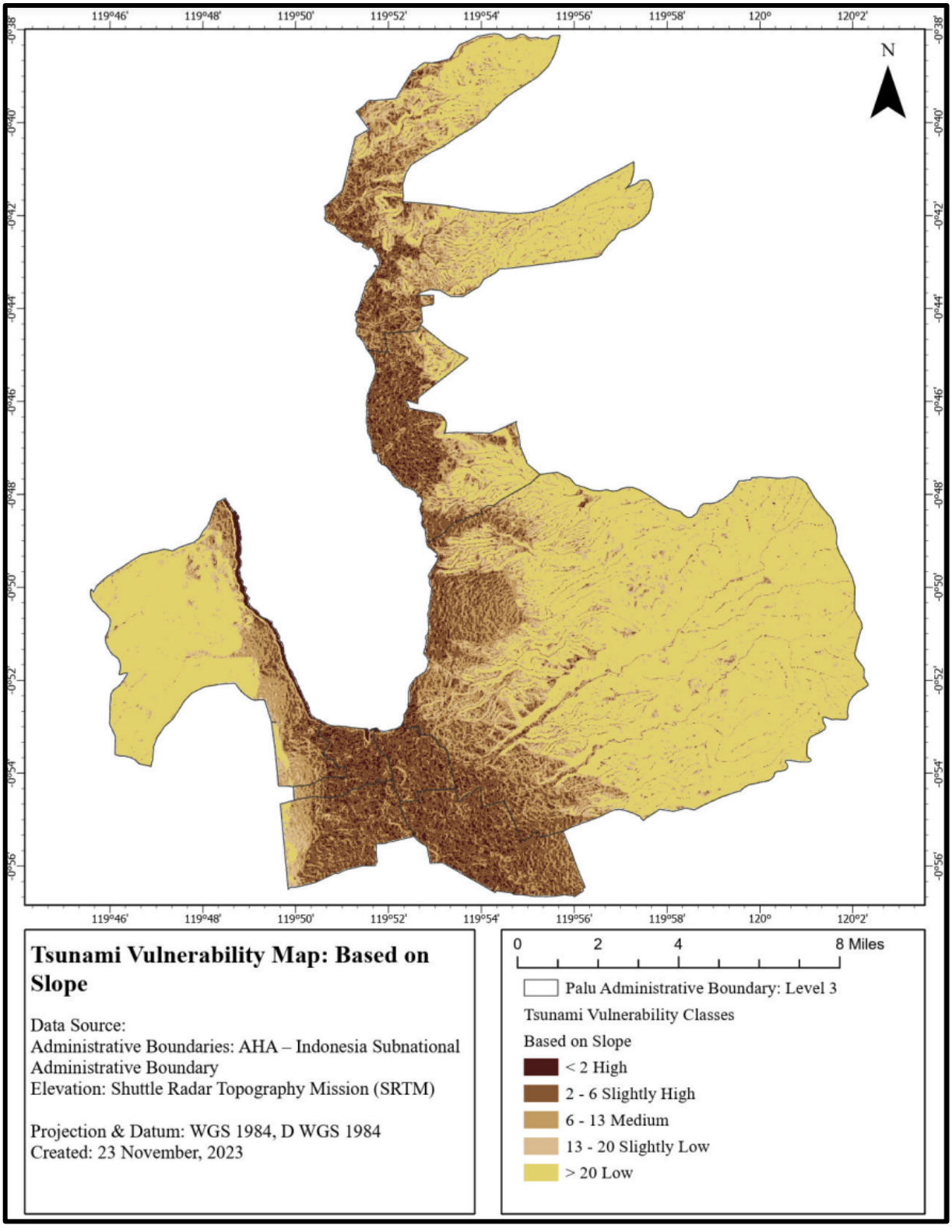


Figure 13 Tsunami Vulnerability Map based on Topographic Slope

6.3 Coastal Proximity Mapping

Distance measurement from coastal line to land using Multiple Ring Buffers with 30m grid was done to create five classes of tsunami vulnerability. To classify coastal proximity, following equation was applied to calculate coastal proximity (Bretschneider& Wybro, 1976):

$$ln\ X_{max} = \ln 1400 + \frac{4}{3} \ln (\frac{Y}{10})$$

Where X_{max} is the maximum reach of the tsunami over land and Y is tsunami height at the coast.

As show in Table 9, a tsunami with a 5-meter run-up can reach up to 556 meters from the shorelines. If the run-up is between 5 to 10 meters, the tsunami can reach between 556 to 1440 meters inland. In the case of run-ups of 10 to 15 meters, the reach extends from 1440 to 2404 meters. For run-up of 15 to 20 meters, the tsunami can cover a distance from 2404 to 3528 meters inland. The pattern follows similarity for higher run-ups. In summary, the five ranges of coastline distance in terms of high, slightly high, medium, slightly low and low vulnerability to tsunami were 0 - 556, 556 - 1400, 1400 - 2404, 2404 - 3528 and over 3528m, respectively. Tsunami vulnerability based on coastal proximity is shown in Figure 11.

Table 12 Tsunami Vulnerability based on Coastal Proximity

Run-up Height (m)	Coastal Proximity (m)	Tsunami Vulnerability
5	0 - 556	High
5 – 10	556 - 1400	Slightly High
10 – 15	1400 - 2404	Medium
15 – 20	2404 - 3528	Slightly Low
> 20	3528	Low

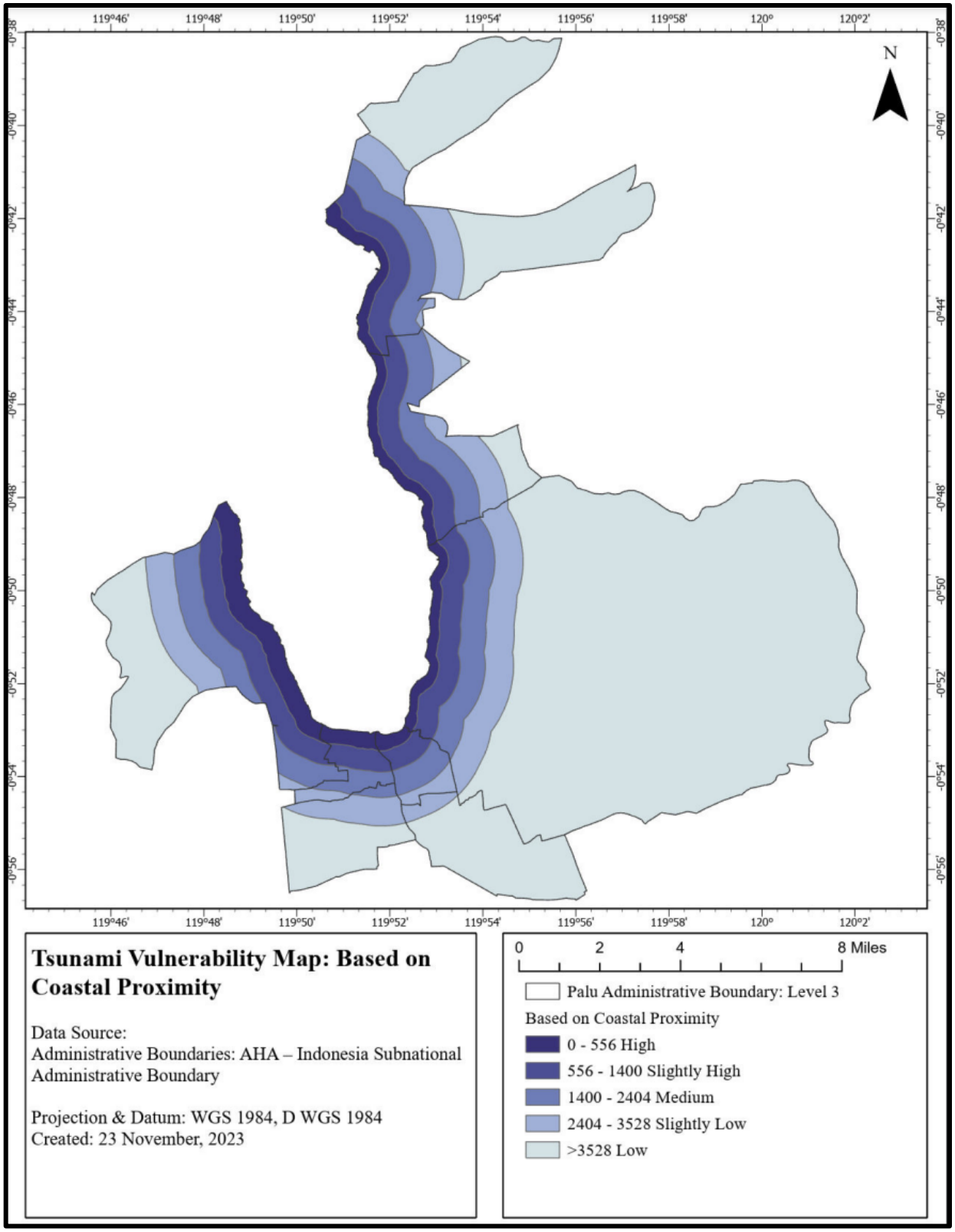


Figure 14 Tsunami Vulnerability Map Based on Coastal Proximity

6.4 Land Use Mapping

The Sentinel-2 land cover includes 14 distinct classes, including forested areas, farmlands, and urban regions. In order to align these classes with the five unique classes of vulnerability, we have merged certain similar categories, as shown in Table 10. For example, forested areas, grasslands, and woodlands have been consolidated into a single forest/shrub class. As shown in Figure 12, urban areas, depicted in red, are classified as having high vulnerability and constitute the largest contiguous sections, suggesting significant population density and infrastructure that may be at risk in the event of a tsunami. The green areas, representing forests, cover vast regions as well but are deemed to have low vulnerability. Lighter shades of red and orange illustrate agricultural and rangeland areas with slightly high to medium vulnerability, interspersed throughout the landscape. Barren lands, marked with a very light red or pink, have a slightly low vulnerability.

Table 13 Tsunami Vulnerability based on Land Use (Sambah & Miura, 2016)

Land Use	**Vulnerability Class**
Urban/Built Areas	High
Agricultures/Crops	Slightly High
Rangeland	Medium
Bare Soil	Slightly Low
Forest/Trees	Low

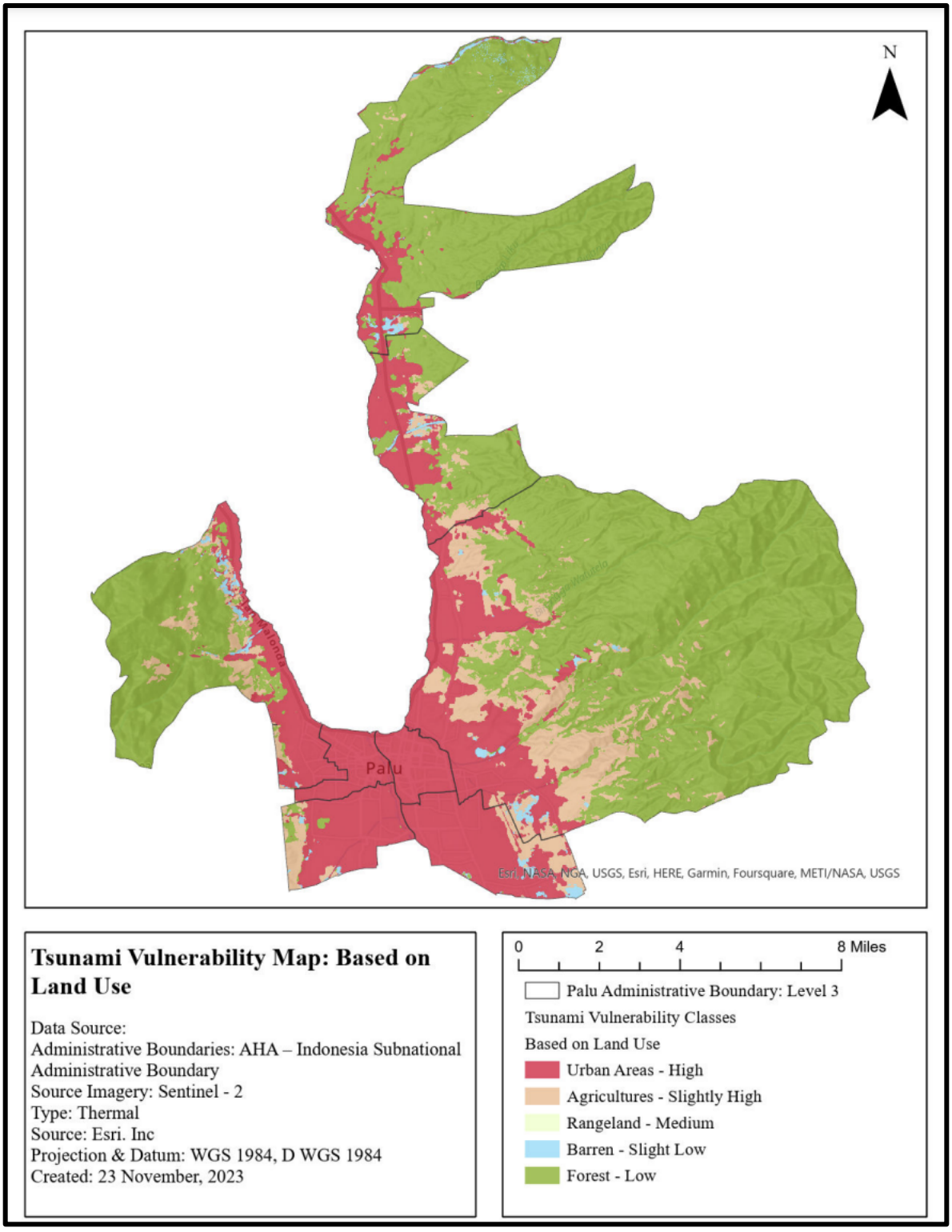


Figure 15 Tsunami Vulnerability Map Based on Land Use

6.5 Analytical Hierarchy Process

The Analytical Hierarchy Process (AHP) is an established decision-making tool used in this study to assign relative importance to factors that affect tsunami vulnerability—elevation, slope, coastal proximity, and land use. To achieve this, a pairwise comparison matrix is utilized where each element is compared with every other element to determine its relative weight in terms of contributing to tsunami vulnerability. The pairwise comparison matrix provided shows the assigned importance of one factor over another, ranging from 1 (equally important) to higher numbers indicating greater importance. For instance, in the matrix, elevation is considered twice as important as slope, and three times as important as both coastal proximity and land use. Table 8 displays the relative weights derived from pairwise comparisons of these parameters. Additionally, hierarchical interactions among these parameters were quantified based on their respective importance, as reflected through numerical scores (from 1 to 9) (Herath and Prato, 2006), also detailed in Table 11.

Table 14 Pairwise Comparison Matrix [8]

Tsunami Vulnerability	Elevation	Slope	Coastal Proximity	Land Use
Elevation	1	2	3	3
Slope	1/2	1	2	2.5
Coastal Proximity	1/3	1/2	1	3
Land Use	1/3	0.4	1/3	1

[8] In the AHP data format, the diagonal line from top right to bottom left is always 1, indicating that the importance of an element compared to itself is always equal. The data in the upper right and lower left corners are in a reciprocal and symmetric format. The numbers represent the relative importance between the indicators, with higher numbers indicating stronger relative importance.

Steps to calculate Weights Using AHP:

1. **Create a pairwise comparison matrix (Table 11):** The matrix compares the importance of each factor against the others on a scale from 1 to 9, where 1 means that both factors are equally important, and 9 means that one is extremely more important than the other.
2. **Calculate the sum of each column in the matrix:** This is done to normalize the matrix.
    - Elevation column sum = $1 + \frac{1}{2} + \frac{1}{3} + \frac{1}{3}$
    - Slope column sum = $2 + 1 + \frac{1}{2} + 0.4$
    - Coastal Proximity column sum = $3 + 2 + 1 + \frac{1}{3}$
    - Land Use column sum = 3 + 2.5 + 3 + 1
3. **Normalize the matrix (Table 12):** Next, we create a normalized matrix by dividing each entry by its column sum. For example, the normalized value for Elevation compared to itself is $\frac{1}{Elevation\ column\ sum}$, and the normalized value for slope compared to elevation is $\frac{2}{Elevation\ column\ sum}$, and so on for each cell in the matrix.

Table 15 Normalized Pairwise Comparison Matrix

Tsunami Vulnerability	Elevation	Slope	Coastal Proximity	Land Use
Elevation	0.46	0.51	0.47	0.32
Slope	0.23	0.26	0.32	0.26
Coastal Proximity	0.15	0.13	0.16	0.32
Land Use	0.15	0.10	0.05	0.11

4. **Average of Rows (Table 13 & Table 14):** Then, for each factor, we calculate the average of its normalized values to determine its weight. For example, for Elevation, we add all the normalized values for Elevation and divide by the number of factors.

Table 16 Normalized Pairwise Comparison Matrix + Weight Calculation

Tsunami Vulnerability	Elevation	Slope	Coastal Proximity	Land Use	Weights
Elevation	0.46	0.51	0.47	0.32	(0.46+0.51+0.47+0.32)/4
Slope	0.23	0.26	0.32	0.26	(0.23+0.26+0.32+0.26)/4
Coastal Proximity	0.15	0.13	0.16	0.32	(0.15+0.13+0.16+0.32)/4
Land Use	0.15	0.10	0.05	0.11	(0.15+0.10+0.05+0.11)/4

Table 17 Variable Percentage Table

Class	Weight Percentage
Elevation	44.096%
Slope	26.653%
Coastal Proximity	18.893%
Land Use	10.358%

5. **Check for consistency:** The AHP process includes a consistency check to ensure that the comparisons made in the matrix are logically sound. This is quantified by the Consistency Ratio (CR), which is calculated using a Consistency Index (CI) and a Random Index (RI). The formula for CR is:

$$CR = (\frac{CI}{RI})$$

CI (Consistency Index) measures how consistent the judgments have been when compared to a large set of possible judgments. It is calculated using the formula:

$$CI = \frac{\lambda \max - N}{N - 1}$$

Where λmax is the largest eigenvalue of the matrix and N is the number of factors.

RI (Random Index) is a value that represents an estimate of the CI one would expect to get by chance. For a matrix of size 4, the RI is typically 0.890.

As shown in Table 15, a CR of 0.056 indicates a satisfactory level of consistency (generally, CR values below 0.1 are considered acceptable). This suggests that the judgments or comparisons made are coherent and reliable. (Saaty 1977; Forman and Selly 2001).

Table 18 Consistency Level Table

CI	RI	CR	Consistency Result
0.05	0.890	0.056	Pass

6.6 Tsunami Vulnerability Mapping

Table 19 Vulnerability Class Based on Elevation (Iida, 1963), Slope (Van Zuidam, 1983), Coastal Proximity (Bretschneider and Wybro, 1976) and Land Use (Sambah & Miura, 2016)

Elevation (m) Weight: 44.096%	Slope (% rise) Weight: 26.653%	Coastal Proximity (m) Weight: 18.893%	Land Use Weight:10.358%	Vulnerability Class
< 5	0 – 2	0	Urban/Built Areas	High
5 – 10	2 – 6	556	Agricultures/Crops	Slightly High
10 – 15	6 – 13	1400	Rangeland	Medium
15 – 20	13 – 20	2404	Bare Soil	Slightly Low
> 20	> 20	> 3528	Forest/Trees	Low

The Analytical Hierarchy Process (AHP) results indicate that elevation is the most critical factor in tsunami vulnerability, accounting for 44.096% of the significance. It is followed by slope at 26.653%, coastal proximity at 18.893%, and land use at 10.358%. These factors, weighted accordingly in ArcGIS Pro, have been used to produce the final tsunami vulnerability map, which is displayed in Figure 13.

As shown in Figure 13, the areas of highest vulnerability are predominantly located along

the coastal regions and extend into the central part of Palu, reflecting the increased risk in zones where a tsunami can have direct and immediate impact due to lower elevation and proximity to the sea. As one moves away from the coast and into regions with varied topography and land use, the vulnerability gradually diminishes.

The map is a comprehensive tool for emergency management, showcasing the gradation of risk across different terrains and guiding the development of targeted strategies for evacuation and other safety measures. It's produced with data from a subnational administrative boundary authority and is intended for use in disaster risk reduction planning.

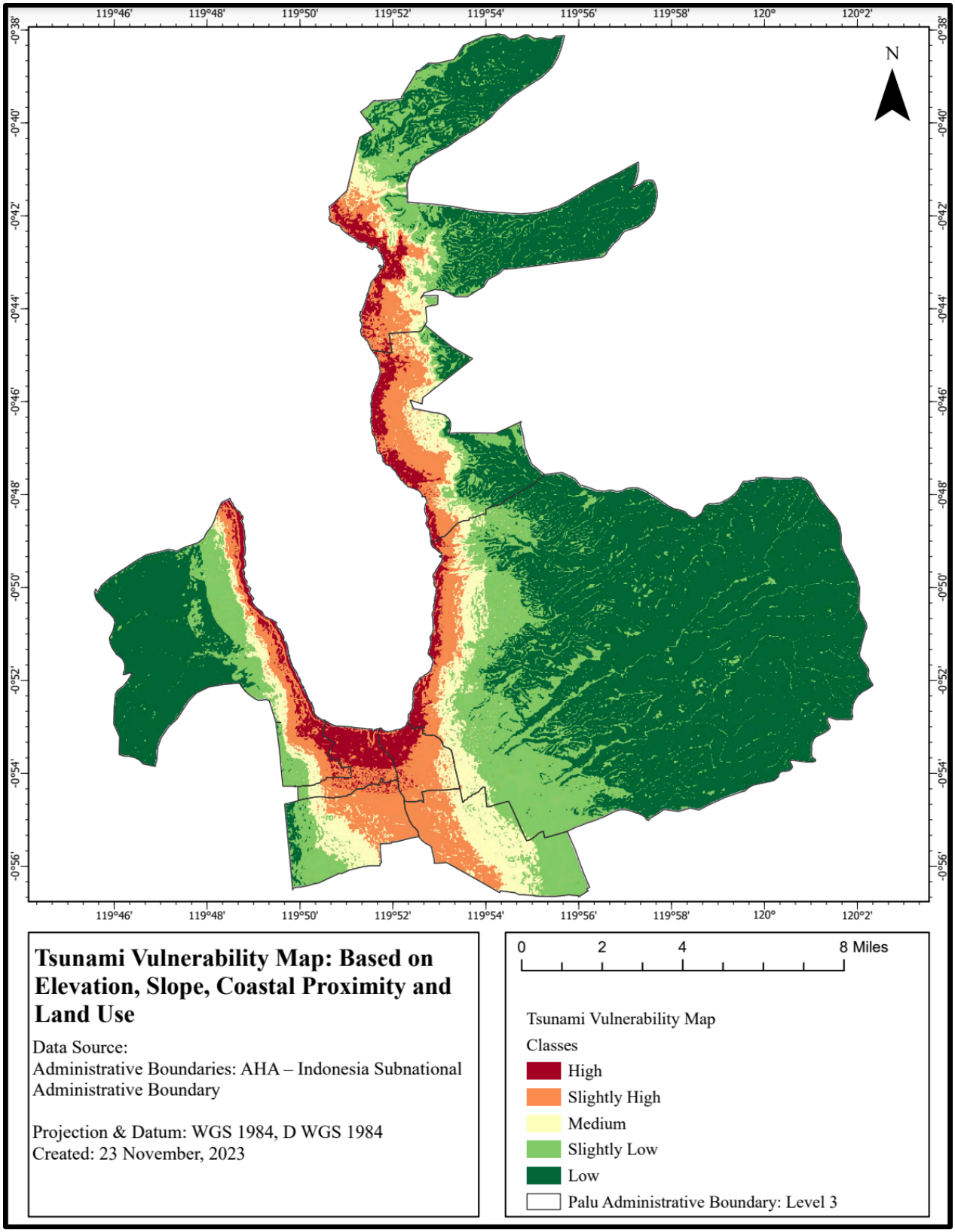


Figure 16 Tsunami Vulnerability Map based on Elevation, Slope, Coastal Proximity and Land Use

CHAPTER 7 SUMMARY

7.1 Conclusion

The Remote sensing techniques used in this thesis are meant to capture the imprint of tsunamis in the post-disaster landscape. This thesis has successfully demonstrated the application of remote sensing techniques in mapping tsunami-affected areas in Palu, highlighting the capabilities of Sentinel-2 imagery in disaster assessment. The use of dNDVI, dNDSI, and dNDWI indices has allowed for a quantifiable measure of the changes in vegetation, soil moisture, and water bodies, providing a clear demarcation of the tsunami's impact. Moreover, the study has underscored the critical role of elevation, slope, coastal proximity, and land use in defining tsunami vulnerability. This multidimensional geospatial approach offers a comprehensive understanding of disaster impacts, informing better preparedness and response strategies.

The tsunami inundation and vulnerability maps show significant overlap, indicating that areas most affected by the tsunami are located in the urban center, low-lying regions, and along the coast. Despite the Analytic Hierarchy Process (AHP) method being somewhat subjective, its validation against the tsunami inundation map confirms the importance of topography, slope, and land use as critical factors in tsunami research. The integration of geospatial variables with field observations have also shed light on the intricate dynamics of tsunami damage. This synthesis of data types provides a more nuanced understanding of vulnerability and the effectiveness of disaster management policies in place. The findings suggest that while early warning systems are essential, they must be coupled with community-based education and infrastructure planning to reduce tsunami risk effectively.

7.2 Policy Implications

The study's findings highlight the need for urban planning that integrates resilience against natural disasters. Policies should focus on the development of infrastructure in vulnerable coastal cities like Palu, emphasizing disaster-resistant construction and strategic placement to minimize damage. In addition, there is an urgent need for the establishment of advanced early warning systems and optimized evacuation routes. Policies should prioritize the integration of technological advancements in tsunami detection and public alert systems, ensuring timely and effective evacuation and response capabilities. This includes developing more effective communication strategies to disseminate early warnings to the public, particularly in remote and rural areas.

The effective use of remote sensing and GIS technologies in this study underscores their potential in disaster management. Policies should support the investment in and utilization of these technologies for better disaster preparedness, risk assessment, and recovery planning. Moreover, the thesis suggests the necessity for coordinated efforts among various governmental and non-governmental organizations in disaster management. Policy frameworks should encourage inter-agency collaboration and sharing of resources and information for efficient disaster response and recovery.

Finally, ongoing research and development in the field of disaster science, particularly in areas prone to natural disasters like Indonesia, should be a policy priority. This includes funding research initiatives and encouraging partnerships between academic institutions, government agencies, and international organizations.

7.3 Limitations

While this study has provided significant insights, several limitations must be acknowledged. Firstly, the spatial resolution of remote sensing data, while sufficient for broad assessments, may not capture finer details necessary for micro-scale planning. This limitation points to the need for higher resolution data or supplementary ground truthing for more detailed analysis. Secondly, the remote sensing data for this study, with only five-day interval between pre- and post-tsunami images, presents a unique dataset. However, such timely data acquisition is not always feasible, as obtaining simultaneous pre- and post-event images is often not possible in many scenarios. Thirdly, the research does not encompass broader socio-demographic variables, such as population density, age distribution, and levels of educational attainment, which could significantly influence vulnerability and resilience in the face of natural disasters.

Additionally, the study's focus on Palu may limit the generalizability of findings to other regions with different geographical and socio-economic contexts. Future research could address these constraints by incorporating a broader range of case studies and employing more sophisticated remote sensing technologies as they become available.

7.4 Recommendations for Future Research

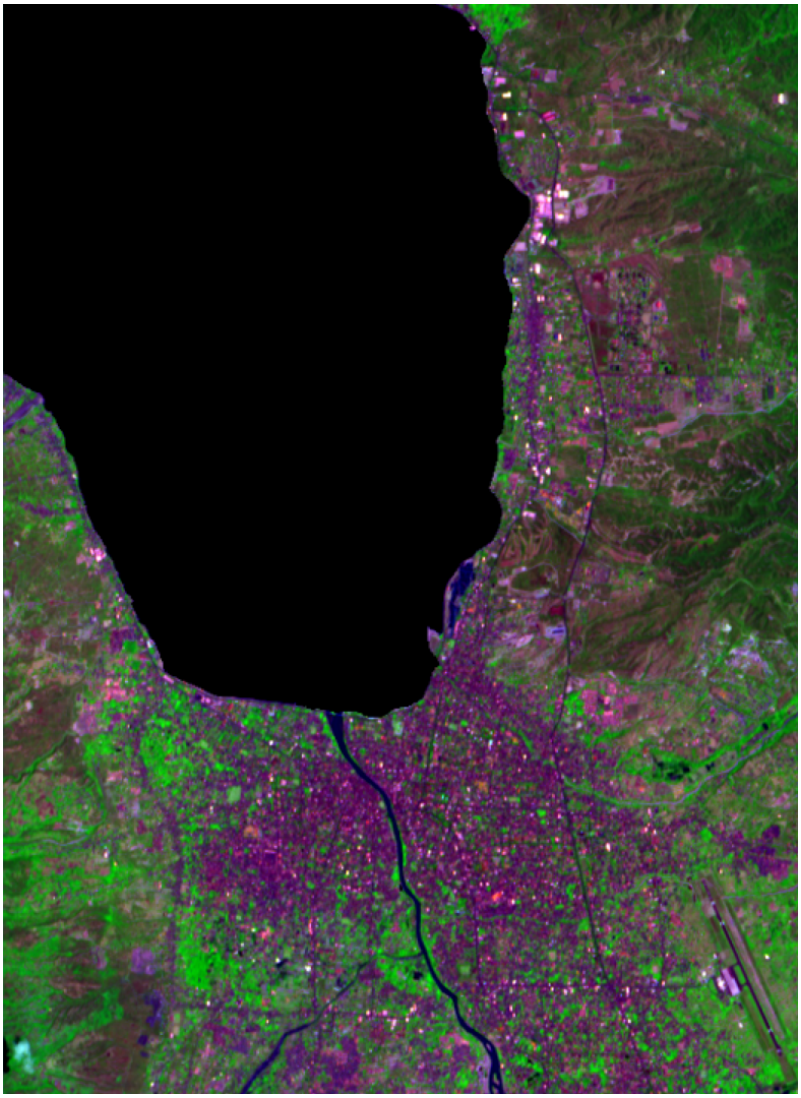
Overall, it would be crucial to deepen the geospatial analysis to observe the environmental recovery patterns over time. A study on the socio-economic impacts, particularly on the rehabilitation efforts and policy effectiveness, could provide critical insights into disaster management efficiency. Additionally, comparative analyses with other disaster-affected regions could shed light on diverse strategies and their success rates across different sociocultural landscapes.

A significant gap remains in understanding the long-term health impacts of the tsunami on survivors. Future research should address both the physical and psychological aftermath, examining the long-term effects on mental health and the efficacy of intervention programs. Innovations in technology, such as the application of drones and artificial intelligence for disaster response, present new frontiers for exploration. These could dramatically transform damage assessment and recovery processes.

Moreover, evaluating the policy responses and institutional structures in place during the disaster would offer a reflective perspective on the strengths and shortcomings of the current disaster management frameworks. Understanding community dynamics and the role of participatory approaches in disaster preparedness could also inform more resilient community engagement strategies. Lastly, assessing the impact of educational initiatives could help in crafting improved training programs for disaster preparedness, ultimately fostering a culture of resilience.

APPENDIX

Appendix 1: False Color Composite



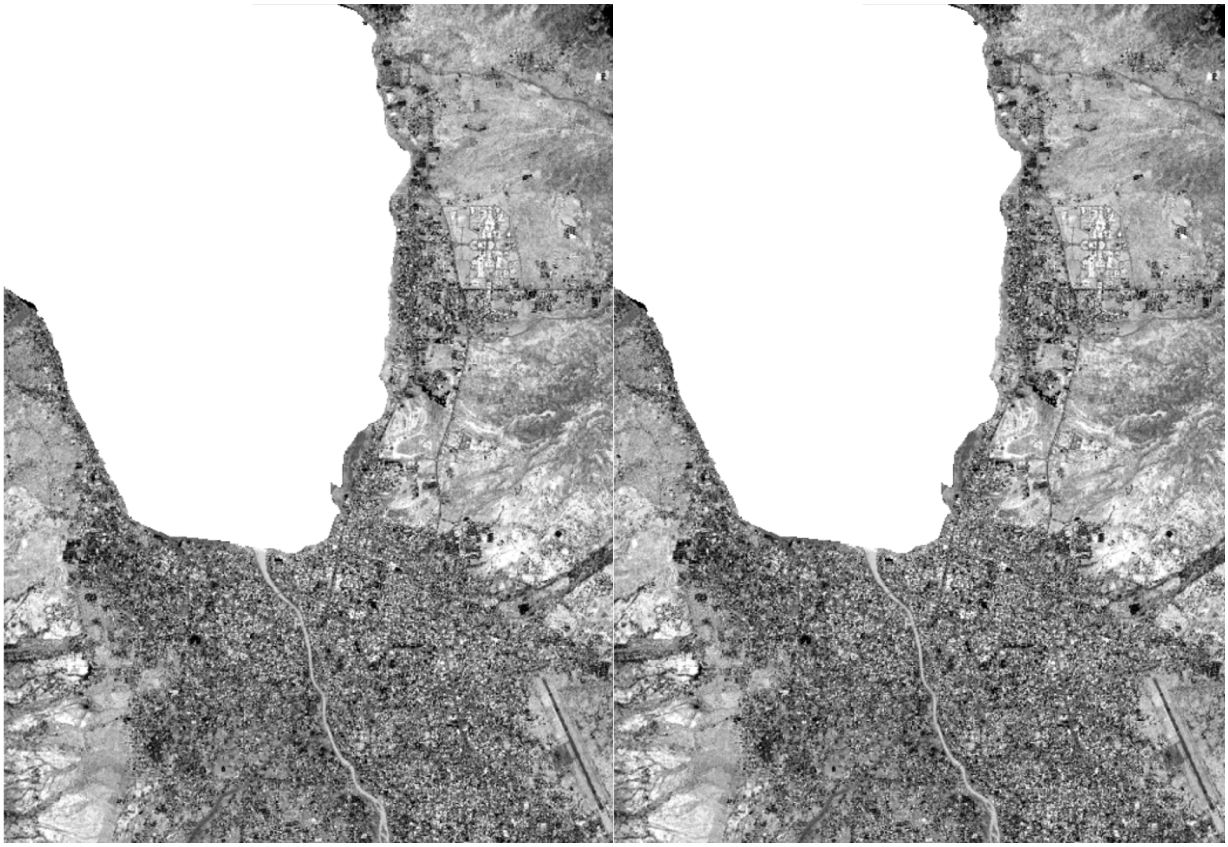
Appendix 2: NDVI Pre-tsunami Image (09/27/2018)



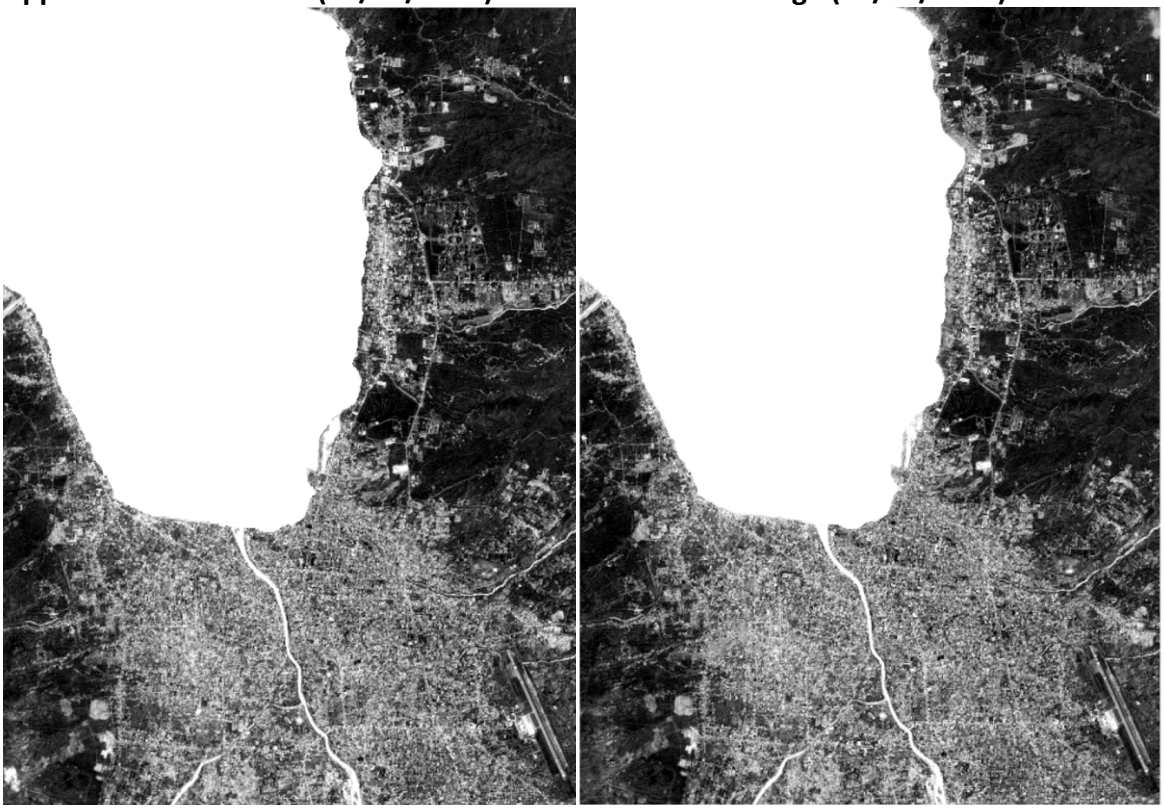
Appendix 3: NDVI Post-tsunami Image (09/27/2018)



Appendix 3: NDSI Pre- (09/27/2018) and Post-tsunami Image (10/02/2018)



Appendix 4: NDWI Pre- (09/27/2018) and Post-tsunami Image (10/02/2018)



BIBLIOGRAPHY

Achmad, W. (2023). The Effectiveness of Earthquake Disaster Management Policy in Indonesia. *Ganaya: Jurnal Ilmu Sosial dan Humaniora, 6*(2), 367-377.

Al-Doski, J., Mansor, S. B., & Shafri, H. Z. M. (2013). NDVI differencing and post classification to detect vegetation changes in Halabja City, Iraq. *IOSR Journal of Applied Geology and Geophysics*, *1*(2), 01-10.

Ananda, J., & Herath, G. (2009). A critical review of multi-criteria decision making methods with special reference to forest management and planning. *Ecological economics*, *68*(10), 2535-2548.

Andrade, C., Ramalho, G., & Teodoro, A. (2019). "Integrating remote sensing data in GIS for tsunami hazard mapping and risk assessment". ISPRS International Journal of Geo-Information, 8(5), 220.

Asoka Kumara, T. (200 6). "Satellite remote sensing applications in tsunami affected area mapping: A case study from the 2004 Indian Ocean Tsunami". International Journal of Remote Sensing, 27(12), 2339-2346.

Atkinson, C., & Curnin, S. (2020). Sharing responsibility in disaster management policy. *Progress in Disaster Science*, *7*, 100122.

Baba, T., & Cummins, P. R. (2005). Contiguous rupture areas of two Nankai Trough earthquakes revealed by high-resolution tsunami waveform inversion. *Geophysical Research Letters, 32*(8).

Banai, R. (1993). Fuzziness in geographic information systems: contributions from the analytic hierarchy process. International Journal of Geographical Information Systems, 7(4), 315-329.

Borrero, J. C. (2005). Field survey of northern Sumatra and Banda Aceh, Indonesia after the tsunami and earthquake of 26 December 2004. *Seismological Research Letters*, *76*(3), 312-320.

Bhola, V., Hertelendy, A., Hart, A., Adnan, S. B., & Ciottone, G. (2023). Escalating costs of billion-dollar disasters in the US: Climate change necessitates disaster risk reduction. *The Journal of Climate Change and Health*, *10*, 100201.

Bretschneider, C. L., & Wybro, P. G. (1977). Tsunami inundation prediction. In *Coastal Engineering 1976* (pp. 1006-1024).

Brown, G., & Fagerholm, N. (2015). Empirical PPGIS/PGIS mapping of ecosystem services: A review and evaluation. Ecosystem services, 13, 119-133.

Burrough, P. A., McDonnell, R. A., & Lloyd, C. D. (2015). *Principles of geographical information systems*. Oxford University Press, USA.

Chang, C. P., & Zhang, L. W. (2020). Do natural disasters increase financial risks? An empirical analysis. *Buletin Ekonomi Moneter Dan Perbankan*, *23*, 61-86.

Chiroiu, L., André, C., & Rekacewicz, P. (2018). "High-resolution satellite imagery in coastal disaster management: Assessing the 2004 Tsunami impact". Disaster Prevention and Management, 27(5), 578-590.

Damarjati, D. (2018). Management Earthquake and Tsunami Disaster in Palu Indonesia. IJSSHR, Volume 05 Issue 01 January 2022, www.ijsshr.in.

Dyer, J. S. (1990). Remarks on the analytic hierarchy process. *Management science, 36*(3), 249 258.

Esteban, M., Tsimopoulou, V., Mikami, T., Yun, N. Y., Suppasri, A., & Shibayama, T. (2013). Recent tsunamis events and preparedness: Development of tsunami awareness in Indonesia, Chile and Japan. *International Journal of Disaster Risk Reduction, 5,* 84-97.

Feizizadeh, B., & Blaschke, T. (2013). Land suitability analysis for Tabriz County, Iran: a multi criteria evaluation approach using GIS. *Journal of Environmental Planning and Management, 56*(1), 1-23.

Geneletti, D. (2004). A GIS-based decision support system to identify nature conservation priorities in an alpine valley. *Land Use Policy, 21(*2), 149-160.

Gonzalez, M., & Medina, R. (1999). Probabilistic Model for Tsunami-Wave Elevation along the Alboran Seacoast. In *Coastal Engineering 1998* (pp. 1168-1181).

Gokon, H., Koshimura, S., & Matsuoka, M. (2017). "Remote sensing-based assessment of tsunami vulnerability and risk in coastal areas". International Journal of Disaster Risk Reduction, 22, 487-501.

Han, S. C., Sauber, J., & Luthcke, S. (2010). Regional gravity decrease after the 2010 Maule (Chile) earthquake indicates large-scale mass redistribution. *Geophysical Research Letters, 37*(23).

Harbitz, C. B., Løvholt, F., Pedersen, G., & Masson, D. G. (2006). Mechanisms of tsunami

generation by submarine landslides: a short review. *Norwegian Journal of Geology/Norsk Geologisk Forening, 86*(3).

Horn, B. K. (1981). Hill shading and the reflectance map. *Proceedings of the IEEE, 69*(1), 14-47.

Indonesia, CNN. "BNPB UNGKAP Tiga Bencana Indonesia Sebagai Fenomena Langka." Nasional, 31 Dec. 2018, www.cnnindonesia.com/nasional/20181231163920-20-357573/bnpb-ungkap-tiga-bencana-indonesia-sebagai-fenomena-langka.

Jaumé, S. C., & Sykes, L. R. (1999). Evolving towards a critical point: A review of accelerating seismic moment/energy release prior to large and great earthquakes. *Seismicity patterns, their statistical significance and physical meaning,* 279-305.

Juwitasari, R., By, Novio, E. B. C., Inpin, W., & Marks, D. (2022, March 23). Disaster Management in Indonesia: Complex challenges of a dual early warning system: Heinrich Böll Foundation: Southeast Asia Regional Office. Heinrich-Böll-Stiftung. https://th.boell.org/en/2022/03/23/disaster-management-indonesia

Lavigne, F., Paris, R., Grancher, D., Wassmer, P., Brunstein, D., Vautier, F., ... & Fachrizal. (2009). Reconstruction of tsunami inland propagation on December 26, 2004 in Banda Aceh, Indonesia, through field investigations. *Pure and Applied Geophysics*, *166*, 259-281.

Liu, P. L., Lynett, P., & Fernando, H. (2015). "Observation of the 2011 Tohoku tsunami using satellite SAR data". Remote Sensing of Environment, 159, 202-215.

Løvholt, F., Pedersen, G., Harbitz, C. B., Glimsdal, S., & Kim, J. (2015). On the characteristics of landslide tsunamis. *Philosophical Transactions of the Royal Society A: Mathematical, Physical and Engineering Sciences, 373*(2053), 20140376.

Kanamori, H. (1972). Mechanism of tsunami earthquakes. *Physics of the earth and planetary interiors, 6*(5), 346-359.

Kanamori, H. (1972). Mechanism of tsunami earthquakes. *Physics of the earth and planetary interiors, 6(*5), 346-359.

Keerthiratne, S., & Tol, R. S. (2017). Impact of natural disasters on financial development. *Economics of Disasters and Climate Change*, *1*(1), 33-54.

Kellenberg, D. K., & Mobarak, A. M. (2008). Does rising income increase or decrease damage risk from natural disasters?. *Journal of urban economics*, *63*(3), 788-802.

Kouchi, K. I., & Yamazaki, F. (2007). Characteristics of tsunami-affected areas in moderate resolution satellite images. *IEEE Transactions on Geoscience and Remote Sensing*, *45*(6), 1650-1657.

Kreimer, A. (2001). Social and economic impacts of natural disasters. *International Geology Review*, *43*(5), 401-405.

Malczewski, J. (2006). GIS-based multicriteria decision analysis: a survey of the literature. International journal of geographical information science, 20(7), 703-726.

Muhari, A., Diposaptono, S., & Imamura, F. (2007). Toward an integrated tsunami disaster mitigation: Lessons learned from previous tsunami events in Indonesia. *Journal of natural disaster science, 29(*1), 13-19.

Mutaqin, B. W., Lavigne, F., Hadmoko, D. S., & Ngalawani, M. N. (2019, April). Volcanic eruption-induced tsunami in Indonesia: A review. In I*OP Conference Series: Earth and Environmental Science* (Vol. 256, No. 1, p. 012023). IOP Publishing.

National Oceanic and Atmospheric Administration. (2021). 2021 U.S. billion-dollar weather and climate disasters: A historical perspective. Climate.gov. Retrieved from https://www.climate.gov/news-features/blogs/beyond-data/2021-us-billion-dollar-weather-and-climate-disasters-historical

Omira, R., Dogan, G. G., Hidayat, R., Husrin, S., Prasetya, G., Annunziato, A., ... & Yalciner, A. C. (2019). The September 28th, 2018, tsunami in Palu-Sulawesi, Indonesia: A post-event field survey. *Pure and Applied Geophysics, 176*, 1379-1395.

Oth, A. (2013). On the characteristics of earthquake stress release variations in Japan. *Earth and Planetary Science Letters, 377,* 132-141.

Paris, R., Lavigne, F., Wassmer, P., & Sartohadi, J. (2007). Coastal sedimentation associated with the december 26, 2004 tsunami in lhok nga, west banda aceh (Sumatra,indonesia). *Marine Geology*, *238*(1-4), 93-106.

Papadopoulos, G. A., Gràcia, E., Urgeles, R., Sallares, V., De Martini, P. M., Pantosti, D., ... & Papageorgiou, A. (2014). Historical and pre-historical tsunamis in the Mediterranean and its connected seas: Geological signatures, generation mechanisms and coastal impacts*. Marine Geology, 354,* 81-109.

Paulik, R., Gusman, A., Williams, J. H., Pratama, G. M., Lin, S. L., Prawirabhakti, A., ... & Suwarni, N. W. I. (2019). Tsunami hazard and built environment damage observations from Palu City after the September 28 2018 Sulawesi earthquake and tsunami. *Pure and Applied Geophysics, 176,* 3305-3321.

Pratama, R. I., & Roza, D. (2019). Peran Badan Penanggulangan Bencana Daerah Dan Pemadam

Kebakaran (Bpbdpk) Kota Padang Dalam Penanggulangan Kebakaran. *UNES Journal of Swara Justisia, 2*(1), 89-104.

Reid, J. A., & Mooney, W. D. (2023). Tsunami occurrence 1900–2020: A global review, with examples from Indonesia. *Pure and Applied Geophysics, 180*(5), 1549-1571.

Rustan, A., & Firdaus, F. (2011). Ancaman Bencana dan Kebijakan Penanganannya di Daerah. *Jurnal Borneo Administrator*, *7*(1).

Samad, M. A., Ali, M. N., & Khairil, M. (2021). Indonesian Disaster Governance: Public Policy and Social Economic Impact. *Elementary Education Online*, *20*(5), 73-73.

Sambah, A. B., & Miura, F. (2016). Spatial data analysis and remote sensing for observing tsunami-inundated areas. *International Journal of Remote Sensing*, *37*(9), 2047-2065.

Sambah, A. B., & Miura, F. (2016). Spatial data analysis and remote sensing for observing tsunami-inundated areas. *International Journal of Remote Sensing*, *37*(9), 2047-2065.

Saaty, T. L. (2008). Decision making with the analytic hierarchy process. *International journal of services sciences*, *1*(1), 83-98.

Shuto, N., & Fujima, K. (2009). A short history of tsunami research and countermeasures in Japan. *Proceedings of the Japan Academy, Series B, 85*(8), 267-275.

Suciani, A., Islami, Z. R., & Zainal, S. (2018, April). " Smong" as local wisdom for disaster risk reduction. In *IOP conference series: earth and environmental science* (Vol. 148, No. 1, p. 012005). IOP Publishing.

Supriatna, J. (2018). Konservasi Biodiversitas: Teori dan Praktik di Indonesia. *Jakarta: Yayasan Pustaka Obor Indonesia.*

Tang, L., Titov, V., & Chamberlin, C. (2016). "Assessment of potential tsunami impact for Southern California, USA using satellite altimetry data". *Natural Hazards, 82*(1), 359-370.

Thiel Jr, C. C., & Zsutty, T. C. (1987). Earthquake characteristics and damage statistics. *Earthquake Spectra, 3*(4), 747-792.

Trias, A. P. L., & Cook, A. D. (2021). Future directions in disaster governance: Insights from the 2018 Central Sulawesi Earthquake and Tsunami response. *International Journal of Disaster Risk Reduction*, *58*, 102180.

Valkaniotis, S., Ganas, A., Tsironi, V., & Barberopoulou, A. (2018). A preliminary report on the

M7.5 Palu earthquake co-seismic ruptures and landslides using image correlation techniques on optical satellite data. National Observatory of Athens, Institute of Geodynamics.

Van Dorn, W. G. (1984). Some tsunami characteristics deducible from tide records. *Journal of physical oceanography, 14*(2), 353-363.

van Rijsingen, E., Lallemand, S., Peyret, M., Arcay, D., Heuret, A., Funiciello, F., & Corbi, F. (2018). How subduction interface roughness influences the occurrence of large interplate earthquakes. *Geochemistry, Geophysics, Geosystems, 19*(8), 2342-2370.

Van Zuidam, R. A. (1983). Guide to Geomorphologic aerial photographic interpretation and mapping. *International Institute for Geo-Information Science and Earth Observation, Enschede, The Netherlands*, *325*.

Wesnousky, S. G. (2008). Displacement and geometrical characteristics of earthquake surface ruptures: Issues and implications for seismic-hazard analysis and the process of earthquake rupture. *Bulletin of the Seismological Society of America, 98*(4), 1609-1632.

Yamazaki, F., Matsuoka, M., Warnitchai, P., Polngam, S., & Ghosh, S. (2005). Tsunami reconnaissance survey in Thailand using satellite images and GPS. *Asian Journal of Geoinformatics*, *5*(2), 53-61.

Yamazaki, F., Matsuoka, M., & Koshimura, S. (2018). "Environmental impacts of the 2011 Tsunami: A study using multi-temporal satellite images". Remote Sensing of Environment, 204, 808-823.

Yeh, C. T., & Huang, S. L. (2009). A GIS-based decision support system for analysis of urban growth management and planning development sustainability. Journal of Geographical Systems, 11(3), 301-324.